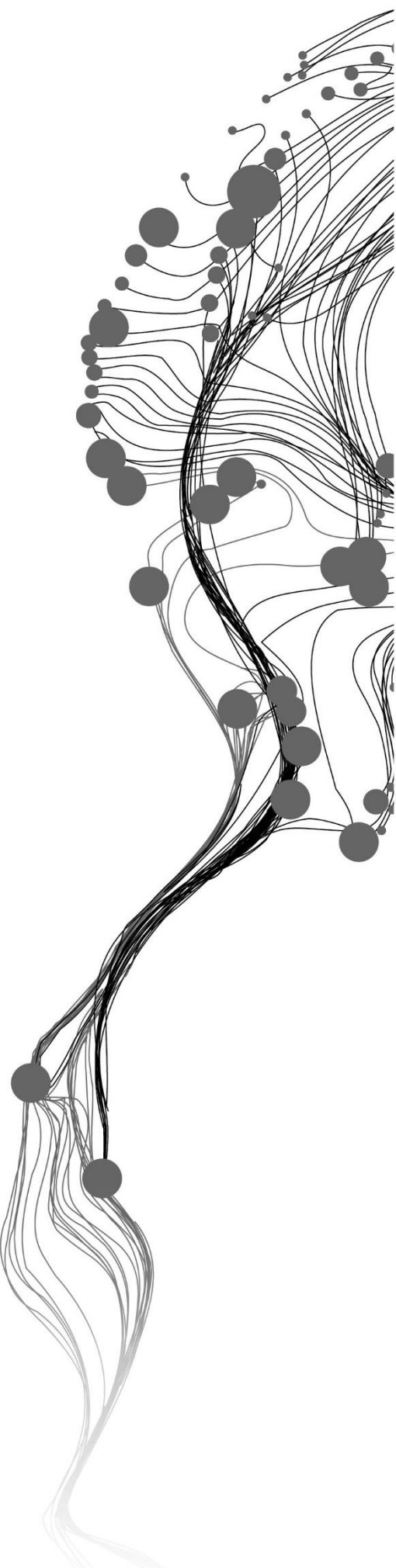# Mapping water constituents in the Liao River Delta in China, using Radiative transfer model and Sentinel 2 MSI images

XIAOHAN ZHANG
06,2021

SUPERVISORS:
DR.IR. Suhyb Salama
DR. Yijian Zeng

MAPPING WATER CONSTITUENTS IN THE LIAO RIVER DELTA IN CHINA, USING RADIATIVE TRANSFER MODEL AND SENTINEL 2 MSI IMAGES

XIAOHAN ZHANG
Enschede, The Netherlands, 06, 2021

Thesis submitted to the Faculty of Geo-Information Science and Earth Observation of the University of Twente in partial fulfilment of the requirements for the degree of Master of Science in Geo-information Science and Earth Observation.
Specialization: Water resources and environmental management

SUPERVISORS:
DR.IR. Suhyb Salama
DR. Yijian Zeng

THESIS ASSESSMENT BOARD:
prof. dr. D. van der Wal (Chair)
prof. Fang Shen (External Examiner, East China Normal University)
ir. A.M. van Lieshou (Procedural advisor)

ABSTRACT

Coastal water bodies and inland reservoirs are typical Case Ⅱ water bodies. Due to the influence and restriction of some factors, such as topography and climate, the local water constituents' conditions are relatively complicated. This has led to the slow development of research on the three constituents of watercolor in this category and has become remote sensing difficulties of ocean color. The currently known water constituents concentrations inversion models mainly include empirical models and semi-analytical models, but for the Case Ⅱ water bodies, the establishment of ocean color models for turbid water bodies has a great advantage. Therefore, the contribution point in its research is the application of an analytical inversion model and the atmospheric correction of the water constituents data.

The study area is located in the Liao River delta, connected to the Bohai Sea, and belongs to Panjin City and Yingkou City, Liaoning Province. There are two main rivers, Shuangtaizi River and Daliao River, with aquaculture, farming, and shipping as the main industries. Affected by the turbidity of the water body, the water constituents concentrations (WCCs) inversion in this area has seen little progress. To fill this gap in the Liao River Delta, this study uses a fully analytical model—2SeaColor (Salama & Verhoef, 2015) to derive three water constituents concentrations of Chlorophyll-a (Chl-a), Non-algal suspended particulate matter (SPM) and Colored dissolved organic matter (CDOM). These WCCs are fundamental in explaining the relationship between the observed reflectance and the inherent optical properties (IOPs). In this study, the long-term series of WCCs derived from Sentinel-2 MSI L1C data was conducted to understand the variability of these WCCs in the study area. The atmospheric correction ACOLITE was used for this purpose. Combined with the field sampling data, the synchronous optimization inversion of the three elements of watercolor in the sea area is realized. The main findings of this article are as follows:

First, the specific inherent optical properties (SIOPs) in the Liao River delta have been derived. 61 in situ water quality data sampled in September 2019 were used to simulate the SIOPs in the Liao River delta, including the absorption coefficient a^*_{chla} of chlorophyll-a(Chl-a) and the power parameter p, the backscattering coefficient of suspended matter (SPM)$b^*_{b_{spm}}$, and the absorption coefficient weight k of colored soluble organic matter (CDOM). And R² values of the inversion WCCs are 0.57, 0.60, and 0.69, respectively, which confirms that the above parameters are suitable for the inversion of the concentration of these constituents in the Liao River delta.

Second, the model estimated accuracy from the satellite has been assessed. Ten Sentinel-2 MSI L1C images after the atmospheric correction during the wet and normal water level periods from 2016 to 2020 were used to obtain the remote sensing reflectance and process five years of water quality monitoring. At the same time, the accuracy of the 2SeaColor model was verified with remote sensing image data synchronized with the satellite and the ground, and the R² values of these three constituents were simulated to be 0.50, 0.60, and 0.61, respectively. It is believed that the model is suitable for remote sensing inversion with Sentinel-2 as the background data. It is applied to do the inversion of the WCCs in a long time series and draw the watercolor inversion diagram.

Third, spatiotemporal variation and mathematic statistics have been analyzed. Based on the retrieval of WCCs in these past five years, it was confirmed that the concentration of the three constituents presents a spatial distribution characteristic of high concentration near shore and low concentration far shore, and gradually decreasing from north to south. The results show that the WCCs have little inter-annual variation and great seasonal variation during these five years. It was also analyzed that the open water and inland reservoirs present opposite seasonal changes. High concentration in the normal water period and low concentration in the wet period for open water, but low concentration in

normal period for the inland reservoirs. According to the different characteristics of geographical location, six sub-regions were zoned and compared for the annual average concentrations. At the same time, the influence factors and potential pollution sources were analyzed, and it is concluded that Chl-a in the Liao River delta is greatly affected by the discharge of aquaculture and farming wastewater, while SPM and CDOM are affected by the water exchange rate, and SPM carries CDOM and hovers in the water body, resulting in similar spatial and temporal changes of these two. Besides the contribution of the fine-scale inversion map to this study, the influence of meteorological factors, including rainfall, strong wind, and cloudy, and the fishery risk brought by the current WCCs conditions were analyzed.

Key words: 2SeaColor; Water constituents concentrations inversion; Liao River delta; Sentinel-2; Chlorophyll-a; Non-algal suspended particulate matter; Colored soluble organic matter.

ACKNOWLEDGEMENTS

TABLE OF CONTENTS

LIST OF FIGURES

LIST OF TABLES

1.   INTRODUCTION

This section explains the necessity of the water constituents monitoring in the case 2 coastal areas, and justifies the importance of chlorophyll-a (Chl-a), colored dissolved organic matter (CDOM), and non-algal suspended particulate matter (SPM). The Liao River delta in China is taken as an example for clarifying the research difficulties in monitoring the water constituents in Case Ⅱ water and explaining the statement of the water quality in this study area. The literature review shows the research status, and research objectives and questions are based on the gap of these studies.

1.1.   Background and Justification

Coastal areas are generally an excellent ecological environment, suitable for human habitation, conducive to the economic development of the "essence of the region"(Dan et al., 2015). Sixty percent of the world's population lives in coastal areas and 100 kilometers from the coast (Cohen, 1997). Therefore, coastal areas influence human activities strongly. There are up to 12 coastal provinces in China. China's eastern coastal regions account for 43.5% of the total water resources (Song et al., 2015). Especially for the Liao River, located in the South of Liaoning province, connected with the Bohai Sea, the river utilization rate is as high as 65% (Song et al., 2015). Liao River has a giant catchment basin in Northeast China, accounts for 232000 square kilometers. The length of this river is about 1345 kilometers, which is the main river system in Northeast China. Affected by industrial development, aquaculture, port trade, and human activities, Liao riverine waters have become increasingly polluted(H. Zhao et al., 2016). For many years, the comprehensive pollution index in the Liao River has been among the top in China, and it is the key basin of national river management(Danfen Zhou, 2015; H. Zhao et al., 2016). In addition to the shortage of plants has increased the sediment supply from land to the riverbed, thereby reducing its water transport capacity and increasing flooding potential.

Water quality conditions are determined by the interaction of water, suspended matter, dissolved matter, aquatic organisms, and sediment. Water constituent concentrations (WCCs) are part of water quality components. It is a series of standards to describe water quality conditions and the degree of water pollution. The water quality monitoring of these three constituents is essential for sustainable development in the Liao River delta region. Also, WCCs are strongly related to the transparency of the river. When the river has a lower content of these three water constituents, the studies of underwater will become easy, such as the water depth and underwater biological detection.

(1) Chlorophyll-a (Chl-a) is the primary pigment that plants need for photosynthesis and is found in most Marine phytoplankton. At present, pollution of coastal environments has become more serious, which causes people's wide attention. Real-time and accurate monitoring of chlorophyll-a is conducive to the risk warning of Marine ecological disasters. Chlorophyll-a concentration reflects the nutrient status of rivers and is a key index for monitoring eutrophication. In addition, the proportion of chlorophyll-a in seawater is closely linked to fisheries and aquaculture(Y. Zhang et al., 2007). The concentration of chlorophyll-a changes obviously with the number of harmful algae in the water,

which has the function of evaluating the density of harmful algae(N. Zhao et al., 2019). It is an important research project for the coastal environment.

(2)Colored dissolved organic matter (CDOM) constantly affects the circulation and biological activities of substances in the water environment. CDOM is mainly discharged from the river band in the inland water bodies and usually has a higher concentration than the seawater, which source from the decomposition and degradation of low and medium plant residues(Y.-L. Zhang et al., n.d.). The change of CDOM concentration is also one of the reasons for the blackening of lake water. The production of CDOM comes from effluent discharge and the death of cyanobacteria and aquatic plants. So it is the significance of the monitoring and analysis of watercolor.

(3)Non-algal suspended particulate matter (SPM) in water has a strong scattering effect on light. They are biological and physical particles. The distribution of the concentration of floating matter directly determines the propagation of light in water, affecting the optical parameters such as the transparency of water and the depth of the true light layer, affecting the thermal budget of the lake, the growth of aquatic organisms, and the primary productivity of water(Kari et al., 2017).
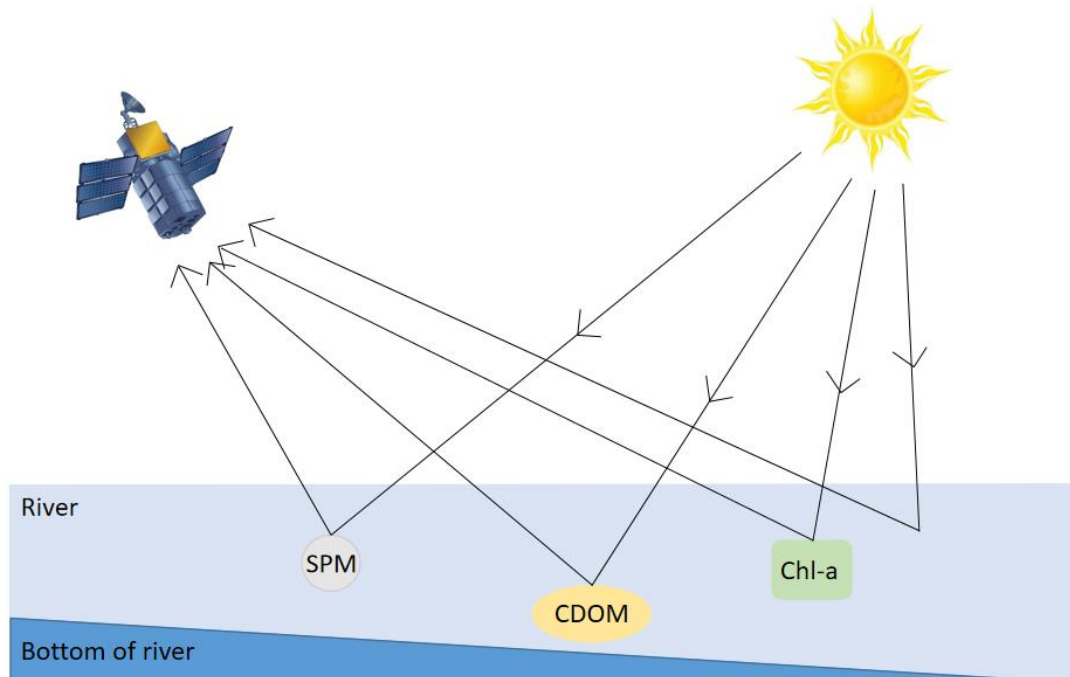
Figure 1: Remote sensing detection of water constituents

In this study, we make use of satellite observations to derive water quality indicators (WQI). However, satellites can merely detect those WQIs that affect the visible light. Therefore this study expresses water quality indicators in terms of some important WCCs that include chlorophyll-a, colored dissolved organic matter, and non-algal suspended particulate matter(Coble et al., 1998). For optimal usability of the riverine waters, each of the water constituents need to be monitor and control. Otherwise, it may influence the local river ecology.

1.2.   Research area problem statement

On the Northwest Coast of the Bohai Sea, these three water constituents are seriously influenced by the two tributaries of the Liao River, the Shuangtaizi River and the Daliao River. Terrestrial source input has been proved to be a crucial source of WCC in the Bohai Sea, which has a particular impact on the coastal waters(Coble et al., 1998). (1)The concentration range of chlorophyll-a is 10-100 ug/m³. The change of sea area and season reflects the growth status of red tide, and its value can be used to judge the algal bloom(Xiaowei Zhang, 2014). Generally, when the concentration above 10 mg/m³, this area can be considered to have a red tide. It always appeared in July and August. (2) The seasonal characteristics of CDOM are high in autumn and low in spring, which is mainly related to the difference of seawater dynamic environment, and the concentration is usually around two m-1. (3) The concentration of SPM influences by the season. The average concentration in the normal water level period and wet period are 57.82 mg/L and 37.41 mg/L, respectively(Fan et al., 2018).

Chl-a, CDOM, and SPM are essential factors of watercolor, which can indicate biophysical status. But researches based on the large region, like the Bohai sea, cannot represent the specific condition of the Liao River delta. Besides, the coastal area river is the typical Case Ⅱ water. These waters are mainly located in places that are particularly affected by the emission of gas and the discharge of wastewaters. Case Ⅱ water is the most closely associated and most threatened by human activities and water pigments. Chlorophyll-a, SPM, and CDOM affect the marine environment. If a reliable evaluation of monitoring WCCs backed up by water color remote sensing data, it would enable us to monitor the effects in real-time, over long periods, and in the coastal region and carry out large-scale studies.

A study on the Liao River delta can overcome the shortfalls of research on nearshore water in the Bohai Sea region, help the local government to make policies to monitor water quality conditions and control water pollution, and then protect the ecological balance of water and the good living conditions of local residents.

1.3.   Literature review

WCCs monitoring is part of water quality assessment. Lots of studies are work on this part. There are some existing conventional methods to get water quality concentrations. The field monitoring method is the traditional way, which is mainly based on sampling the water column in the field. It is based on a statistical method, using a large number of measured data to calculate the relationship between the water leaving reflectance and WCCs. Water sample collection and monitoring are also helpful for the research in the Liao River. The researcher from the Liaoning Hydrology and Water Resources Survey Bureau used the six-year water samples data to show the effectiveness of pollutant control(Xiaowei Zhang, 2014). These in situ measurement data can be collected from the hydrological stations. Although field monitoring is considered as the reference to which validation is performed, it is limited in its spatial and temporal coverage. Especially for the large-scale or long time series monitoring, these data are not enough for the analysis. With the development of satellite technology, WCCs retrieved from the satellite images becomes true. It is a helpful method to get the concentration and save the human resources, compared with the field monitoring. But the field data are still needed for the modeling. The remote sensing retrieval method is divided into two main ways, the empirical algorithm method and the semi-analytical method.

1.3.1. Empirical algorithm method

In recent years, with the Copernicus program of the European Space Agency and the Ministry of Natural Resources of China, remote sensing has shifted to the operational phase of deriving WCCs on a systematic basis. Their typical methods are divided into empirical algorithm methods and semi-analytical(Maritorena et al., 2002). The first method focuses on the single constituent and has proved to illustrate the correlation of the WCC and R_{rs} by algebraic expression(Howard R. Gordon & Morel, 1983). A multiple linear regression model was used to predict water quality parameters from the Landsat multispectral scanner (MSS) data(Carpenter & Carpenter, 1983). (Beck et al., 2016) compared several satellite reflectance algorithms using synchronous synthetic imagery for estimating chlorophyll-a concentration. (Bélanger et al., 2008) derived the ratio of CDOM and total absorption coefficient at 412nm from 307 sites. (Ngoc et al., 2020) gathered 205 coastal and inland stations in situ data to process an empirical band-ratio algorithm for the relation of remote sensing reflectance (R_{rs}) and SPM concentrations in the coastal of Vietnam. Most of the articles reveals the empirical algorithm method needs the strong effort of marine monitoring station support, and the inversion of Chl-a, SPM and CDOM all together is a difficulty.

1.3.2. Semi-analytical method

While the semi-analytical optical models have the ability and convenience to derive multiple WCCs. (H. R. Gordon, 1988) developed a semi-analytical radiance model firstly and used the sea surface upwelled spectral radiance as a function to estimated phytoplankton pigment concentration. (Lee et al., 2002) developed a multiband quasi-analytical algorithm to derive Inherent Optical Properties (IOPs), based on Gordon's model. But these two early methods haven't considered the early saturation condition from the high turbidity water(Salama & Shen, 2010). Some of the researchers focus on the single constituents for the turbid waters, and they also get some improvement for the progress of semi-analytical models. (Jun Chen et al., 2015) built a muti-band semi-analytical algorithm (UMSA) for estimating Chl-a concentration in the Yellow River Estuary in China, which gets good inversion results. The performance of the mixed algorithm turned from (Doxaran et al., 2003; Nechad et al., 2010; Siswanto et al., 2011) original equations formatted by (Han et al., 2016) has been proofed have satisfactory inversion results for SPM in the low-to-midterm and high turbid water. (Zhu et al., 2011) developed a Quasi-Analytical Algorithm(QAA-E) to process the CDOM absorption in the Mexico area, and lots of turned algorithms are based on this principle, like QAA_cj using for Yangtze River in China (Wang et al., 2017). Besides, the radiative transfer model is a new way to describe the relationship between the IOPs and Reflectance(Ronghua et al., 2009). In the case of certain light conditions and surface waves, the variation of Irradiance below the surface of the water is largely determined by important optical substances, such as dissolved substances and suspended substances. Salama and Verhoef were presented a full analytical remote sensing model (2SeaColor) (Salama & Verhoef, 2015) to simulate the chlorophyll-a, CDOM, and SPM concentrations and verified to get high accuracy, and this method has also proved suitable for the turbidity water (Arabi et al., 2016; Yu et al., 2016). The 2SeaColor model is a useful method to do the inversion of Chl-a, SPM, and CDOM altogether, even in the turbid condition, so it is much suitable for the Case Ⅱ water body.

1.3.3.   Multiple remote sensing data application

Multiple satellite sensors are used to estimated WCCs previously. SeaWIFS data were used to retrieve chlorophyll-a, SPM, and CDOM in the coastal area by (Tassan, 1994). Water quality parameters can also be derived from Landsat TM imagery(Kulkarni, 2011). Meris imagery was proposed to monitor and model the water quality(Giardino et al., 2017; Mohamed, 2015). Modis data shows its application for modeling WCCs as well(Jones, 2006). (Jiang Chen et al., 2017) proved Sentinel-2 images have the ability to retrieved Chl-a concentration. Previous studies also proposed Sentinel-2 images that could be used to mapping other water quality parameters. CDOM and SPM were included in their approach(Kutser et al., 2019). But there is still a difficulty in integrating with in situ measurement and satellite data because of the low availability of field and satellite observations and the complexity of coastal areas(Arabi et al., 2020).

Water quality in the Liao River delta is strongly influenced by the surrounding land using and human activities. WCCs are variable with different locations. So a small distance can lead to different water conditions. Phytoplankton is greatly affected by nutrient input from land sources(Tian Hongzhen et al., 2019). Pollutants and sediments exhibit certain randomness by the different land utilization(Qi et al., 2020). Fine-scale water quality analysis is needed for the Liao River, because there are a lot of small tributaries (about 15 meters) that connect the river to the village. Land-use type also influences the WCCs (Nana Feng, 2020). Water quality research on these small features supports the evidence for the water quality condition on the main channel. A multispectral instrument onboard the Sentinel-2 satellite offer a higher spatial resolution that is suitable to resolve the fine-scale of Estuarine water and nearby coastal environment. In this research, the 2SeaColor model will be used to retrieved ocean color constituent concentrations from the sentinel-2 MSI images. A 20-meter resolutions WCCs map will be generated to show the water dynamic difference located in the Liao River delta.

1.4.   Research objectives and research questions

1.4.1.   Research objectives

The research objectives of this research are to (a) analyze the seasonal cycle of WCCs and relate to activities in the upper stream from 2016 to 2020, (b) understand the small scale water dynamics in the Liao River delta, and (c) give the evidence of the possible pollution sources from small feathers and find the water region most affected by human activities.

1.4.2.   Research questions

Based on the research objectives, the following research questions are posted to guide my study.
(1)Technology:
    a. What is the usage of Sentinel 2 MSI images in the process of retrieving WCCs?
    b. What is the accuracy of the 2SeaColor model retrieval WCCs compared with the sampled data?
(2)Science:
    a. What are the spatial and temporal variations of WCCs in the Liao River delta?
    b. How do the small-scale features reveal the water dynamic?
    c. How does the water level during the normal periods and wet periods influence the
    concentrations and absorption of the water constituents?
(3)Application:

a. What Specific Inherent Optical Properties (SIOPs) parameters need to be used in order to retrieve accurate estimates for the concentrations and absorption?

b. What is the accuracy of the 2SeaColor model retrieval WCCs from the Sentinel-2 MSI images?

1.5.   Conceptual framework and technique flowchart

1.5.1. Conceptual framework
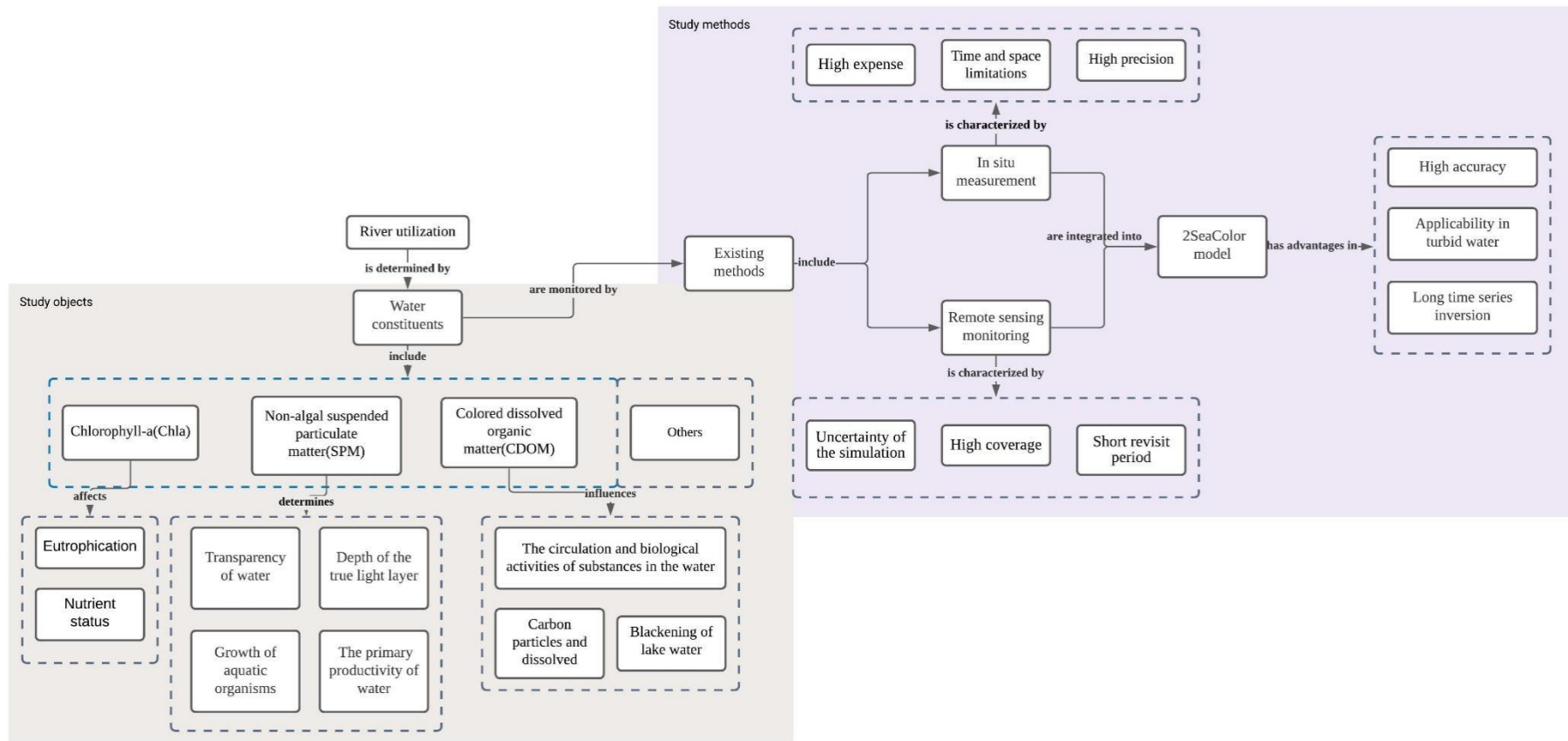
Figure 2: The thesis conceptual framework (the blue dashed boxes identify the focus of this MSc thesis)

1.5.2. Flowchart
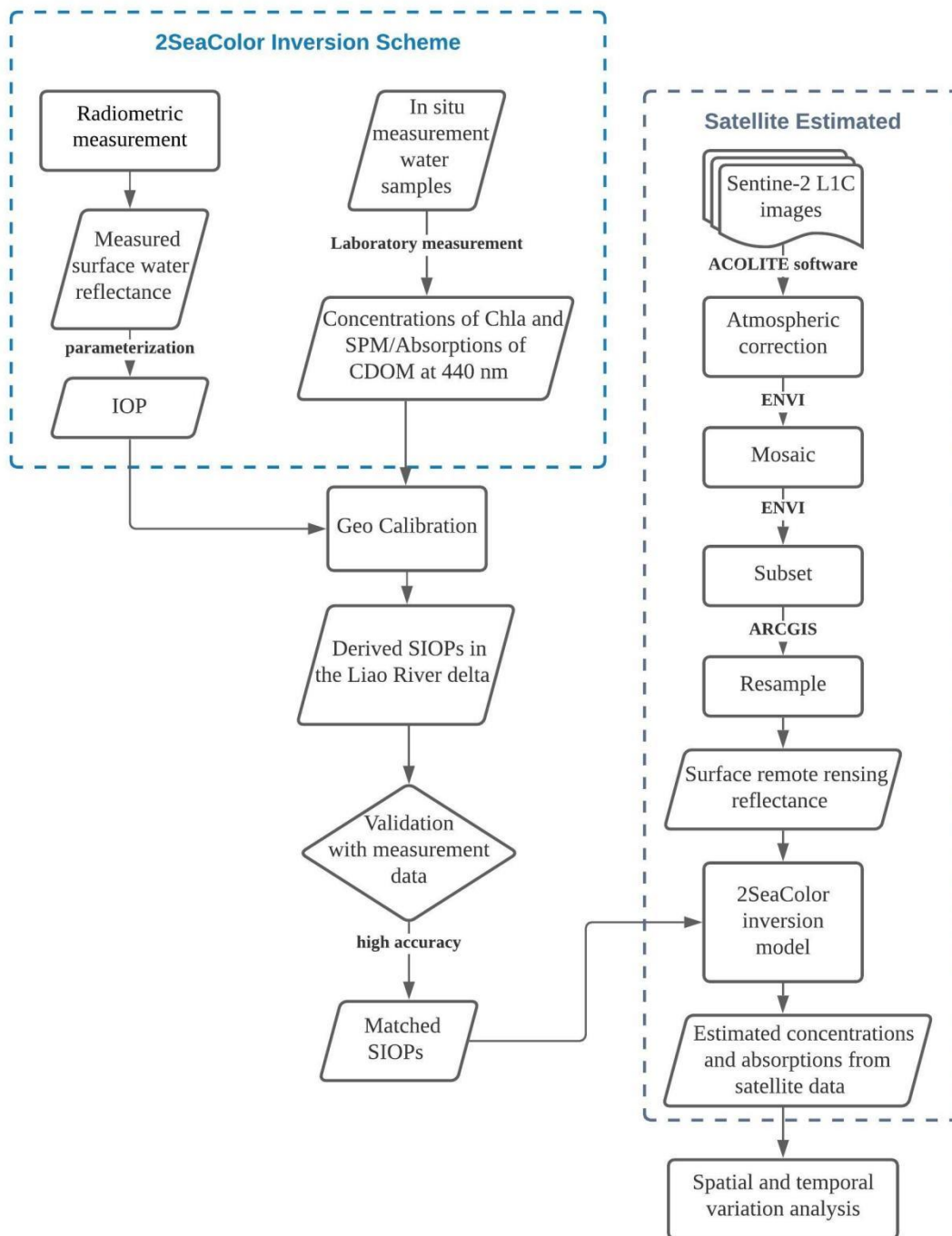
Figure 3: The study flowchart.

Figure 3 is the flowchart in this research. It is mainly divided into two parts. The first part is used the measured data from the fieldwork to derived the SIOPs in the Liao River delta. Some of the SIOPs from the previous literature are based on the Bohai sea. Here the validation is arranged to verify the estimated SIOPs accuracy. The second part is the estimation from the satellite. Satellite surface remote sensing reflectance and SIOPs are the input parameters to retrieve WCCs and absorption. And the data analysis is based on retrieval values.

2.   STUDY AREA AND DATA INTRODUCTION

This section introduces the physical situation in the study area and the information of in situ measurement data and Sentinel-2 satellite images. Besides, pre-processing steps of the Sentinel-2 images in this research were list below.

2.1.   Study area introduction

The Liao River is one of the seven major rivers in China, passes through four provinces in China, including Hebei, Inner Mongolia, Jilin, and Liaoning(SHAO Zhi-Fang et al., 2015), so the water quality in Liao River affects the pass-through provinces. The Liao River delta is located in the southern part of Liaoning Province, is the northernmost end of China's coastline, facing the Bohai Sea, located at longitude from 121°27' to 122°23', and latitude from 40°21' to 41°28' (Qi et al., 2020), The Liao River delta is formed by the accretion of the Shuangtaizi River, Daliao River, Daling River, and Xiaoling River. The Liao estuary is an obvious bell-shaped accumulation estuary, and the wind-wave is the main meteorological factor that influenced the surface undulation. The annual average temperature of the sea surface is 8.3℃ (ZHAO Xue et al., 2018). The delta landform changes frequently, and the largest sediment is Gaizhou shoal.

This research study area is set around the Liao River delta. Two main rivers in this catchment, Shuangtaizi River and Daliao River are both from the Liao River system. The western distributary of this delta is called the Shuangtaizi River. It flows through the Southern edge of Panjin city in Liaoning province and covers an area of 62 square kilometers. About 200,000 people live near this river (Song et al., 2015). Daliao River is located on the east side of the Shuangtaizi River, which is about 40 kilometers away. The catchment of the Daliao River is approximate 1962 square kilometers in Yingkou city in Liaoning province. The main land-use types in the Liao River delta are offshore aquaculture and natural wetland area, causing a severe sediment accumulation nearby.
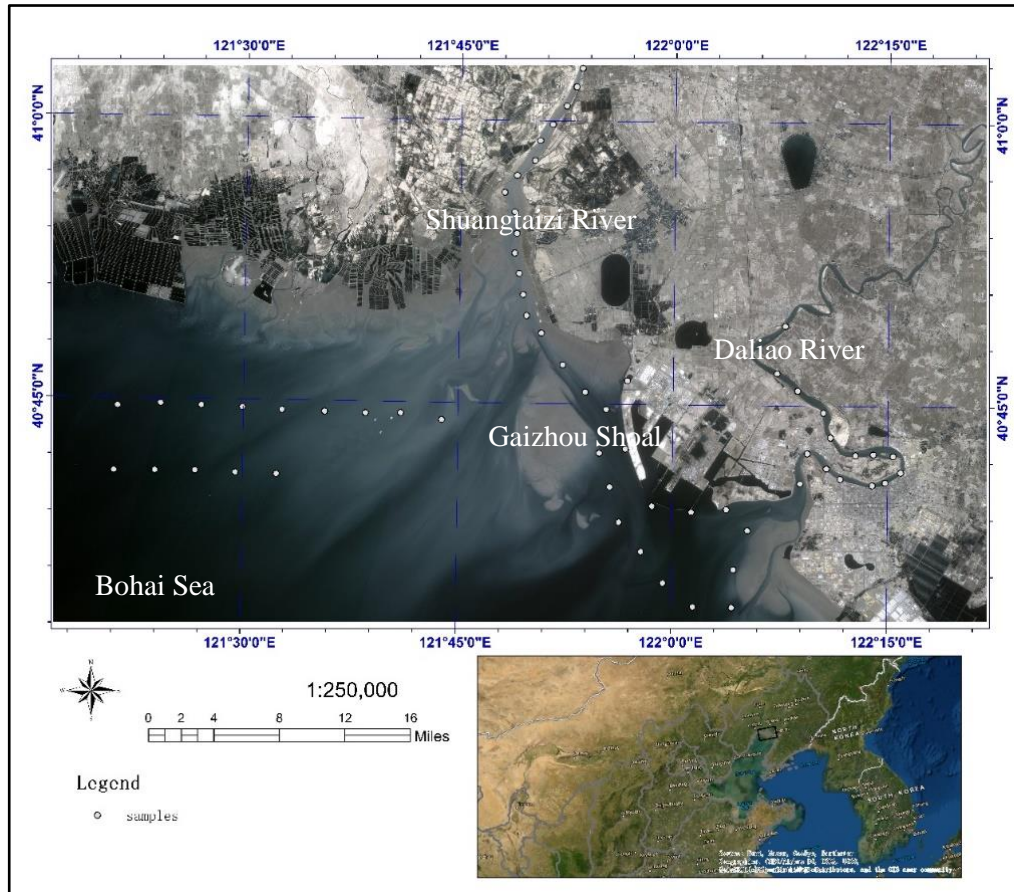
Figure 4: The study area and field sample locations in the Liao Delta, Liaoning Province, China.

2.2.   Existing in situ measurement data

In situ WCCs of Chl-a and SPM data and the absorption of CDOM at 400 nm were measured from September 21 to September 24 in the 2019 wet season. There were 61 water samples, which locations were shown in Figure 1. Sampling points were 2 kilometers equidistant distributed in the study area in the Liao River delta. Fourteen samples were located on the west bank of the estuary, 14 samples were collected on the south bank of the estuary. 15 and 18 samples came from the Daliao River and the Shuangtaizi River, respectively. All of these samples were well protected and sent to a professional laboratory to measure the concentrations of chlorophyll-a and SPM, and the CDOM absorption.

The high precision spectrometer ASD FieldSpec 4 Hi-Res was used as a measuring tool to record the water spectral. A hand-held GPS was used to measure the geographic coordinates synchronously when equidistant water samples were collected below the surface water with a depth of 0.5 meters. Chlorophyll-a, CDOM, and SPM water samples were stored in the appropriate container to prevent damage to the sample. In addition, the three constituents of watercolor were tested in a professional laboratory to get the concentrations of chlorophyll-a and SPM and CDOM absorption at 400 nm, based on the 61 water samples from the Liao River delta.
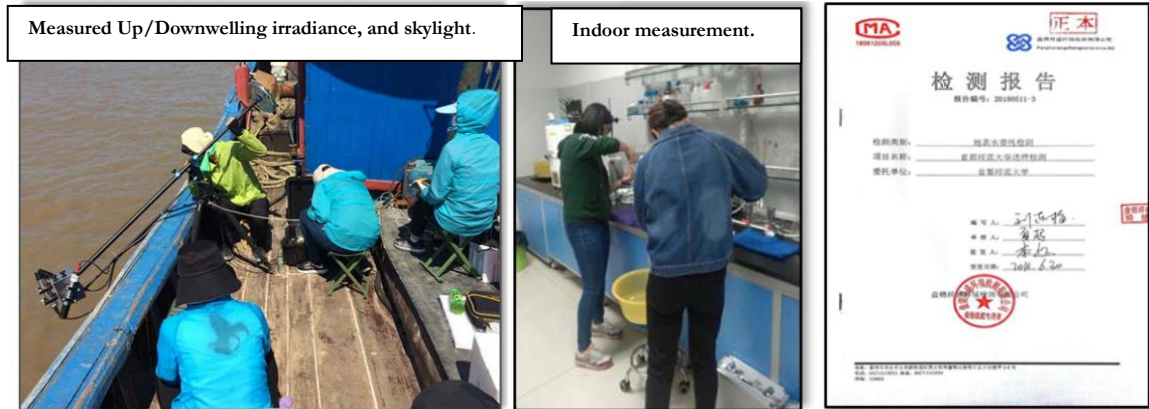
Figure 5: Fieldwork and in situ measurements report.

Table 1: Data collection for the WCCs from the fieldwork.

	Chl-a[ug/m3]	CDOM[m-1]	SPM[mg/l]
Maximum value	40.32	1.91	97
Minimum value	0.52	0.44	7
Median value	4.50	1.04	27
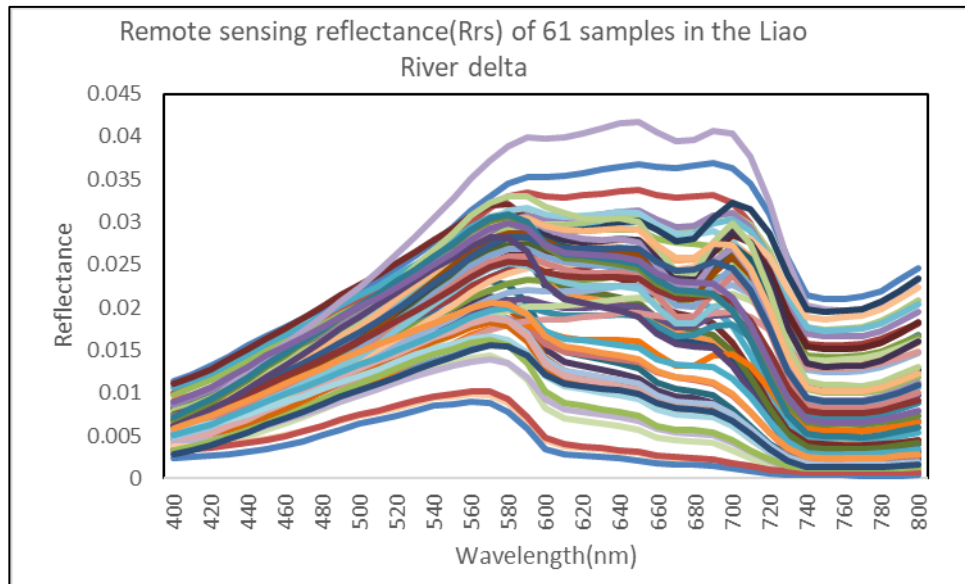
Figure 6: Surface remote sensing reflectance (R_{rs})of water samples recording from the spectrometer.

The 61 measured R_{rs} mean reflectance is the average of 10 measured reflectances for each sample from the spectrometer, and the reflectance shows a little change to the standard water reflectance curve. In the sampling Case Ⅱ water area, Liao river delta, the reflectance steadily grows from 400nm to 560nm, and reaches the first peak at around 570 nm. Later, it goes down slightly until 600nm, then declines with fluctuation. A second peak appears at around 700nm for the multiple samples. After that is a significant decrease and slight upturn from 700 nm to 800nm.

2.3. Sentinel-2 MSI L1C optical satellite images

Only optical sensors can be used to retrieve water constituent concentrations. Sentinel-2 can offer higher temporal, spectral, and spatial resolution satellite images. Therefore it is suitable for geographical and oceanographic research. Sentinel-2 is an Earth observation mission from the Copernicus Project, and it provides a relatively high spatial resolution, from 10 to 60 meters, optical images of land and coastal waters. This mission has two satellites, Sentinel-2A and Sentinel-2B.

Table 2: Wavelengths and Bandwidths of the different Spatial Resolutions of the Sentinel 2 mission (source: https://sentinel.esa.int/web/sentinel/missions/sentinel-2/instrument-payload/resolution-and-swath)

Spatial Resolution (m)	Band Number	S2A		S2B	
		Central Wavelength (nm)	Bandwidth	Central Wavelength (nm)	Bandwidth
10	2	492.4	66	492.1	66
	3	559.8	36	559.0	36
	4	664.6	31	684.9	31
	8	832.8	106	832.9	106
20	5	704.1	15	703.8	15
	6	740.5	15	739.1	15
	7	782.8	20	779.7	20
	8a	864.7	21	864.0	22
	11	1613.7	91	1610.4	94
	12	2202.4	175	218507	185
60	1	442.7	21	442.2	21
	9	945.1	20	943.2	21
	10	1373.5	31	1376.9	31

Water-leaving radiance reflectance, also called remote sensing reflectance (Rrs), is calculated from the Acolite atmospheric correction. In section 2.3, two atmospheric correction methods for the water region are showed to reveal an accurate way to do the data pre-processing.

Table 3: Information of the satellite image used to validate Sentinel-2

	Data Name	Date	Data Level
1	S2B_MSIL1C_20190924T024549_N0208_R132_T51TVF_20190924T053202	2019.9.24	L1C
2	S2B_MSIL1C_20190924T024549_N0208_R132_T51TUF_20190924T053202	2019.9.24	L1C

These two images take the same time as the fieldwork. Therefore, in the 2SeaColor inversion scheme, the mosaic image of these two is used to validate the estimated WCCs results. Also, they are used to test the accuracy of two atmospheric correction methods. The comparison between the in-situ measurement Rrs

and processed Rrs is based on the same time period. In the five years Spatio-temporal variation in section 5, the using ten Sentinel-2 MSI images were listed in Table 9.

2.4.   Atmospheric correction methods comparison

Before the WCCs inversion process, a suitable atmospheric correction method is considered to choose and use for retrieving the R_{rs}. Two common methods for the water region atmospheric correction methods, (a)ACOLITE and (b)C2RCC are compared in this part. (a)ACOLITE is a binary distribution software developed by the Royal Bureau of Natural science in Belgium, for processing the atmospheric correction for Landsat 8 and Sentinel-2 images. The mechanism of ACOLITE is an image-based algorithm, using Gordon's algorithm(Brockmann et al., 2016) results to estimate the radiation leaving the water column (Lw) after correcting the scattering influence from molecular and aerosol in the atmosphere. Based on this assumption, ACOLITE can also retrieve water-leaving reflectance in both the visible and NIR bands together with other parameters of interest in marine and inland waters(Howard R. Gordon & Wang, 1994). (b)Another processor is called Case-2 Regional Coast Colour (C2RCC). It is capable of processing data of Sentinel-2/3, Landsat 8, VIIRS, and other satellite images. C2RCC is available through ESA's Sentinel toolbox SNAP. The neural networks are the basic technology to invert the radiative transfer simulations based on their large database(Bramich et al., 2021).

Table 4: Atmospheric correction methods comparison result.

Band	WaveLength(nm)	C2RCC_R	C2RCC_RMSE (sr-1)	ACOLITE_R	ACOLITE_RMSE (sr-1)
B1	443.9	0.53	0.0049	0.60	0.0056
B2	496.6	0.58	0.0051	0.54	0.0049
B3	560.0	0.54	0.0044	0.58	0.0049
B4	664.5	0.62	0.0065	0.62	0.0055
B5	703.9	0.63	0.0072	0.69	0.0060

The comparison was based on estimated and measured reflectance. Take the reflectance from the ASD spectrometer as the standard values, compared the matching result from ACOLITE and C2RCC. The results show that ACOLITE has a higher matching rate than C2RCC. Therefore, this research took ACOLITE method to do the following Sentinel-2 MSI images atmospheric correction process.

2.5.   Satellite images pre-processing

Sentinel-2 has two available product types for users to download, the top-of-atmosphere reflectance in cartographic geometry (Level-1C) and the bottom-of-atmosphere Reflectance in cartographic geometry (Level-2B). In this research, Level-1C products were used to calculate the IOP and WCCs. The optical images on the last ten-day of a month were downloaded in order to be consistent with the sampling time on September 24 in 2019. The wet water level period (July, August, September) and normal water level period (October, November) images from each year were downloaded separately. Because of the cloud cover influence, all images were minimized the cloud coverage below 10%. Four steps were followed to do the image pre-processing: (a)ACOLITE atmospheric correction, (b)Mosaic, (c)Subset, (d)Resample.

(a) The optical images were used ACOLITE to do the atmospheric correction. The dark spectrum fitting

(DSF) is the main algorithm. The DSF computes atmospheric path reflectance (ϱ path) based on multiple dark targets in the scene or sub-scene, with no a priori defined dark band. The adaptation and applicability of the DSF to Sentinel-2 are described in(Vanhellemont, 2019). And it shows a strong availability and high accuracy for inland water atmospheric correction than the Sen2Cor method(Bramich et al., 2021). After the ACOLITE process, it automatically generates the band images in 10 meters resolution.

(b) Before modeling the water constituents, Sentinel-2 images after atmospheric correction need to be mosaic in the ENVI software. Because a single image only covers 290 kilometers, and a single image cannot cover both the Shuangtaizi River and Daliao River in my research region. The convergence of the two images lies between these two rivers. In this study region, two same days and adjacent satellite orbit images were needed to mosaic first for the following process. Chose the output background value as 0 and used cubic convolution as the mosaic method.

(c) Due to the huge amount pixels slow down the inversion speed of concentrations and absorption. Except for the image on September 24, 2019 (Section 4.2.3, used for comparing the difference between the inversion data and the measured data, because the 61 samples are lay on the full mosaic size), other images were all clipped from the ENVI subset tool. The area within the red box (see Figure 18) is the main study region for analyzing the spatial and temporal changes. The typical landcover features are almost contained in this area. For instance, the main study objects (Shuangtaizi River and the Daliao River) are covered in the region. Also, this area includes lakes, ports, and fishponds.

(d) Considering the speed and efficiency of the 2SeaColor model inversion work, all the bands of Sentinel-2 images were resampled from 10 meters resolution to 20 meters resolution. Although decrease in the resolution will cause an absolute loss of some details. But the width of surrounding tributaries is almost over 10 meters. Therefore 20 meters resolution is acceptable, and this resolution is suitable for processing the further fine-scale resolution concentration maps efficiently. The resampled method is the nearest algorithm.

3. RESEARCH DESIGN AND RESEARCH METHODS

3.1. Research design

(1)Data collection:

   a. The existing in situ measurement data is described in section 2.2.
   b. Sentinel-2 Multispectral Instrument (MSI) level-1 images need to be download from the ESA (https://scihub.copernicus.eu/dhus/#/home). The cloud cover percentage will be set below 10% to ensure that the study area was free of cloud interference. The main study period is from 2016 to 2020. Sentinel-2 L1C images were downloaded monthly from June to November. The reason for excluding other months is the Liao River is frozen in Winter. These images cover the wet and normal stages of water flow. In the Liao River system, the normal water level period is always in November, the wet period and dry period are usually in August and April.

(2)Data processing:

   a. Used the two-stream remote sensing model (2SeaColor)(Salama & Verhoef, 2015) as the research way. Used in situ data and field sampled reflectivity data to calculate SIOPs in the Liao River delta, based on the Geo-calibration and validation and the 2SeaColor model parameterization.
   b. Used above parameters and surface remote sensing reflectance of satellite images to retrieve WCCs of chlorophyll-a, SPM, and CDOM absorption at 400 nm.
   c. Compared the same time period satellite images inversion WCCs and absorption values with the measurement values and validated the accuracy of the 2SeaColor estimated data. Map for concentrations and absorption from 2016 to 2020, and analyzed the spatial and temporal variation of water constituents distributions.

(3)Data analysis:

   a. The accuracy of the 2SeaColor model estimated results from the actual sampling data are planned to use scatter plots and R^2 value, Root Mean Square Error (RMSE), and the Mean Absolute Error (MAE) to present.
   b. Different time period satellite images make the spatial and temporal variation analysis become a reality. The analysis of these three time periods is helpful in studying the seasonal WCCs changes.
   c. Twenty meters resolution WCCs maps show the variability of water dynamics. They are strong supports for finding the most human-activities-influenced water region.

3.2. The 2SeaColor model methodology

The 2SeaColor model was first proposed by Salama and Verhoef in 2014. It is a new hydro-optical model, comprising an analytical forward model and an inversion scheme(Arabi et al., 2020). Two-stream radiative transfer equations are the fundamental theory of this model. And the difference of the 2SeaColor model is to consider the influence of the radiation flux of direct sunlight, as described by(Duntley, 1942). Also, this

model is well known for its high inversion result under high water turbidity conditions(Arabi et al., 2018). Therefore, it is an efficient method for estimating the WCCs from the surface water reflectance, R_{rs}.

3.2.1. 2SeaColor model forward model

The 2SeaColor model forward modeling(Salama & Verhoef, 2015) is listed as follows.

$$R = \frac{E^+(0)}{E_d(0)} = \frac{r_\infty * E^-(0) + r_{sd}^\infty * E_s(0)}{E_d(0)}$$

$$r_\infty = \frac{x}{1 + x + \sqrt{1 + 2x'}}$$

$$r_{sd}^\infty = \frac{\sqrt{1 + 2x} - 1}{\sqrt{1 + 2x} + 2\mu_w}$$

$$R_\infty = (1 - f) * r_\infty + f * r_{sd}^\infty$$

$$R_{rs} = \frac{0.52 * R}{Q - 1.7 * R'}$$

Where:

R is the irradiance reflectance just beneath the surface water.

$E^+(0)$ is the upward diffuse flux, $E^-(0)$ is the downward diffuse flux.

$E_d(0)$ is the total downward flux of diffuse and direct light, $E_s(0)$ is the direct solar flux.

r_∞ is the so-called infinite reflectance.

r_{sd}^∞ is the directional – hemispherical reflectance of the semi-infinite medium.

μ_w is the cosine of the SZA below the (flat) water surface.

f is the fraction of direct light, 0.25.

R_∞ is the diffuse reflectance.

R_{rs} is the calculated water-leaving Reflectance.

x is the ratio of the total backscattering coefficient and the total absorption coefficient b_b/a.

Q is the ratio of the water upwelling irradiance to upwelling radiance just beneath surface, 3.25.

3.2.2. Parameterization and SIOP derivation

$$a = a_{chla} + a_{CDOM} + a_w$$

$$b_b = b_{b,spm} + b_{b,w}$$

Where the subscripts of W, chlorophyll-a, CDOM, and SPM stand for water molecules, Chlorophyll-a, Colored Dissolved Organic Matter, and non-algal suspended particulate matter, respectively. Water molecule absorption and backscattering values are taken from(Mobely, 1994) and(Pope & Fry, 1997). $a_{chla}$and $b_{b,spm}$ are Inherent Optical Properties (IOPs) provided at 440 nm, a_{CDOM} is the absorption at 400 nm.

The chlorophyll-a absorption (a_{chla}) was calculated by applying the equation provided below:

$$a_{chla}(\lambda) = a_{chla}^*(\lambda)C_{chla}^p$$

$$a_{chla}^*(\lambda) = a_{chla}^*(\lambda_{440})NSF(\lambda)$$

Where NSF is the normalized spectral function for Chl-a(de Moraes Rudorff & Kampel, 2012).

The non-algal suspended particulate matter (SPM)(Yu et al., 2016) was calculated as follow:

$$b_{b\,spm}(\lambda) = b_{b\,spm}^{*}(\lambda_{440})C_{spm}(\frac{\lambda_0}{\lambda})$$

The SIOP $a_{chla}^{*}(\lambda_{440})$, power p and $b_{b\,spm}^{*}(\lambda_{440})$ of the Liao River delta are estimated from the derived IOP and measured concentrations.

The absorption of light by CDOM also constitutes an important light interaction in water and plays an important role in the change of the underwater light field. The adsorption of yellow substance is the product of dissolved organic matter concentration and its specific adsorption.

$$a_{CDOM}(\lambda) = a_{CDOM}(440)\exp(-s(\lambda - 440))$$

S is the spectral slope of CDOM. $a_{chla}^{*}(\lambda_{440}), p, b_{b\,spm}^{*}(\lambda_{440})$ and S are the specific inherent optical properties(SIOPs) in the Liao River delta. SIOPs are essential parameters for estimating the Liao River delta water constituents' conditions(Salama & Shen, 2010). Good specific SIOPs are lead to high accuracy inversion results(Ambarwulan et al., 2011).

3.2.3. Inversion scheme

In the 2SeaColor model, five bands (from band1 to band5) of sentinel-2 image reflectance are used to retrieved IOPs from the nonlinear least-squares method simultaneously. The key of the inversion work is mainly to fit the simulated spectrum with the actual spectrum. The actual spectrum is the after atmospheric correction water-leaving reflectance from the Sentinel-2 MSI images. The 2SeaColor model adjusts the initial IOPs to generate the spectrum from itself. When these two spectrums are the best fitting, these IOPs will be recorded. In this research, 'lsqnonlin' is used to solve the data fitting problems after setting the low and up boundaries. The default algorithms 'trust-region-reflective' of the 'lsqnonlin' is used in the research. This algorithm is used to solve the nonlinear least-squares (nonlinear data-fitting) problem.

$$\sum (R_{rs_{obs}} - R_{rs_{model}})^2$$

The calculation is used for all bands.

When 'trust-region-reflective' applicable. The problem must have: objective function includes gradient, only bounds, or only linear equality constraints (but not both). The lower boundary (lb) and upper boundary (ub) of the IOPs in this research are listed below:

lb= [1e-5, 1e-5, 1e-5, 0.0085, 0.1];
ub= [10 ,10, 10 , 0.05, 1.7];

The adjusted IOPs and constant SIOPs coefficients of the Liao River delta are the input parameters to estimate the WCCs. The spatial and temporal variation analysis can be realized based on the inversion scheme of different satellite images.

3.3.   2SeaColor interfaces establishment

This part is working to create the interfaces for doing the inversion quickly and efficiently. All the code was built based on MATLAB APP DESIGNER software. Two different interfaces were constructed in order to fit the various purpose.

Matlab App Designer is a professional tool to create software apps in the programming environment of Matlab. The user is not required to master software designing ability. Easily drag and drop visual components to layout the design of the graphical user interface (GUI) and use the integrated editor to quickly program its behavior. This tool combines two primary tasks of app building into the same environment– laying out the visual components of a GUI and programming app behavior.

3.3.1. Single image processing interface

Figure 7 is the initial interface for processing a single image. This interface provides the image's basic information, like the path and reflectance of different bands. And the concentration of chlorophyll-a and SPM, and absorption of CDOM will be generated as a TIF file and automatically saved in the corresponding folder.

There were six components used in the single image processing interface. (1) The Tab Group was used to create a software background for the app and given the name of "Inversion Scheme". All of the other components were dragged within the tab boundary. (2) The Edit Field Text was used for two purposes– labeling the usage of different components and showing the import path of the images in the blank text box. (3) All of the callback instructions were based on the Button components, including loading the folder path in the text box, reading the import folder, and running the 2SeaColor model function. (4) The Table was a place to display the R_{rs} reflectance. This reflectance was reshaped into one column for one band. Five bands reflectance listed together in the table. And it is a visible tool to reveal the possible errors before the inversion processing. (5) Message Box was called to remind users when the reflectance importing and model inversion were done. (6) The reflectance matching result was shown in the Figure Box to display the differences between the actual spectrum and simulated spectrum for the ground feature pixels. The actual spectrum is the after atmospheric correction water-leaving reflectance from the Sentinel-2 MSI images, and the simulated spectrum is the 2SeaColor model derived best fitting spectrum from the inversion scheme.
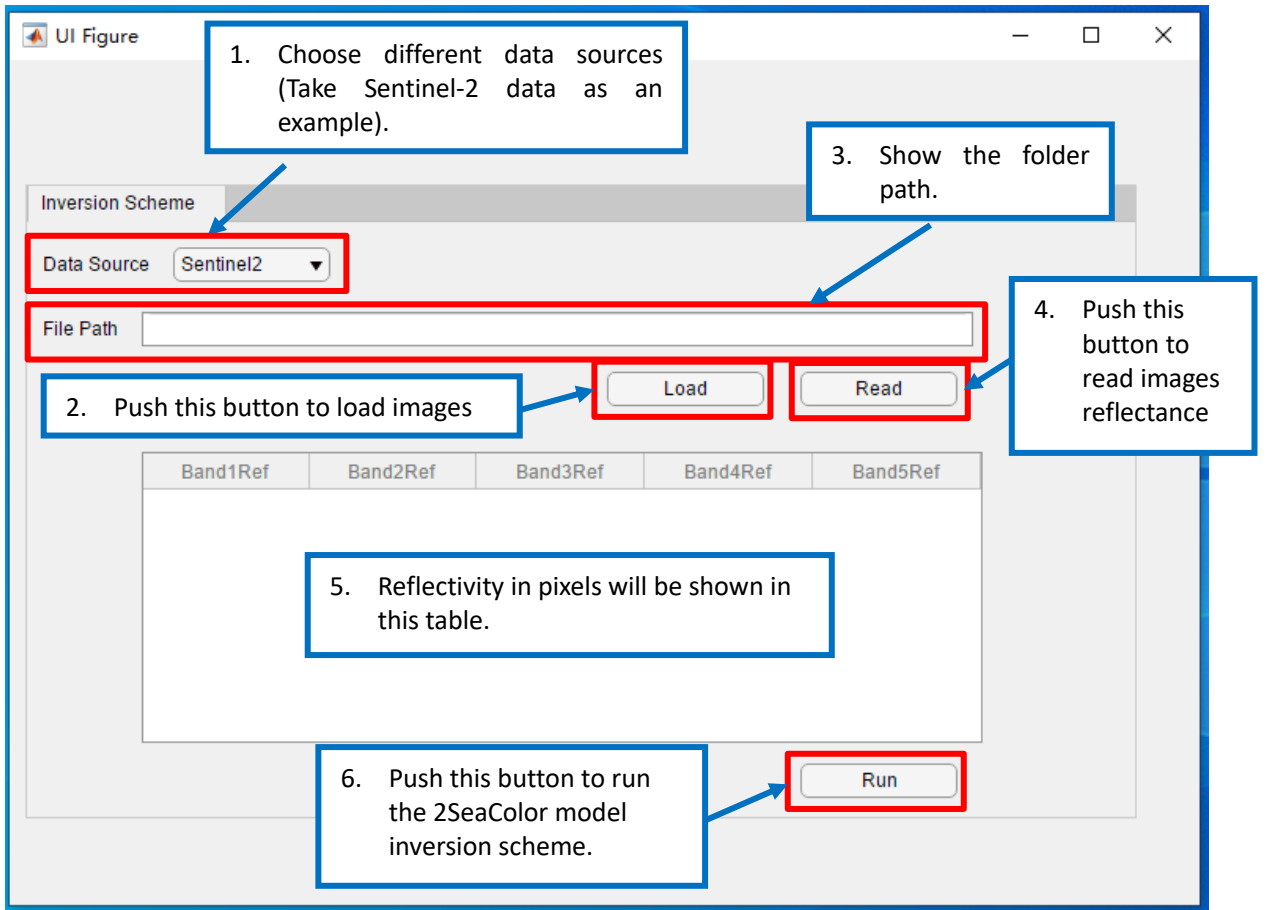
Figure 7: Interface introduction and specific steps of software operation for the single image processing purpose.
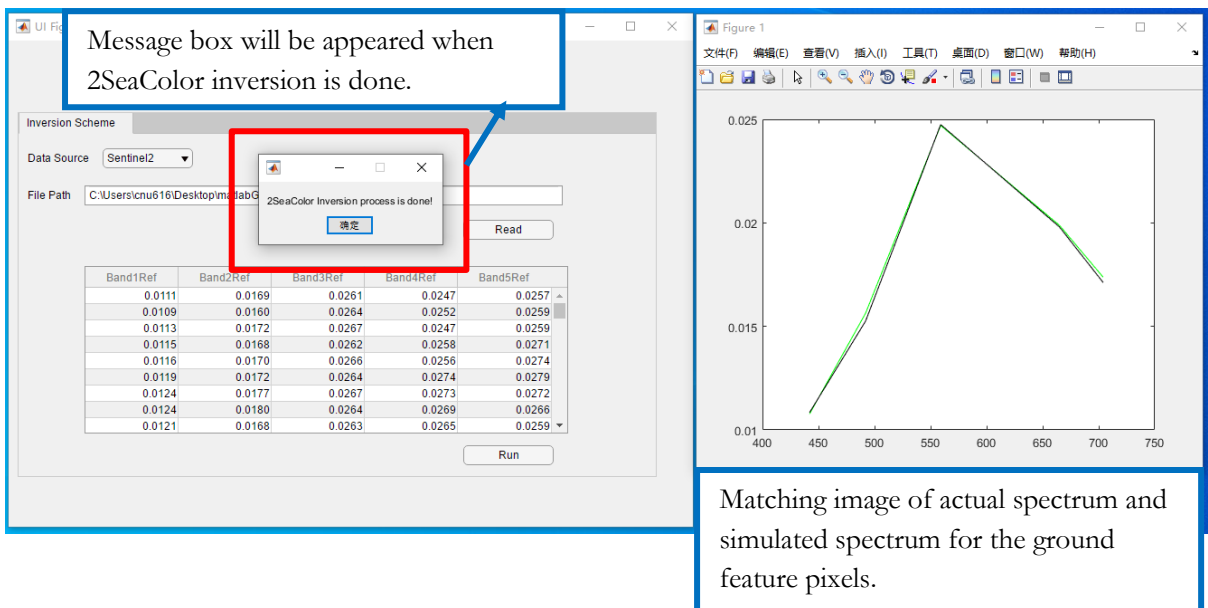
Figure 8: Procedure chart for the single image processing when doing the model inversion.

cdom	2020/12/30 10:34	TIF 文件	5 KB
chla	2020/12/30 10:34	TIF 文件	5 KB
spm	2020/12/30 10:34	TIF 文件	5 KB

Figure 9: The generated TIF file is automatically saved in the corresponding folder.

3.3.2. Batch images processing interface

Figure 10 is the initial interface for processing the batch images. This interface is similar to the single image processing interface, and most of the functionality is the same as that, but it is simplified from the former. Take three different periods of images. For example, three subfolders, with Sentinel-2 images respectively, were stored in the main folder. The information of the main folder is shown in Figure 11. And the processing was processed one by one. After all the processing was done, a message box was appeared to remind the inversion was finished, see Figure 11. And the concentration of chlorophyll-a and SPM, and absorption of CDOM will be generated as a TIF file and automatically saved in the corresponding subfolders.

In order to realize batch images processing function, FOR loop statement was used to traverse the task structure, identify and read subfolders images in turn to participate in the calculation. A matrix set is constructed to store multi-band reflectance. The key code is as follows:

image_name = imgDir(1).name;

image = imread(strcat(file_path,image_name));

[row,col]=size(image);

B=zeros(row,col,img_num);

B(:,:,1)=image;

for j = 2:img_num

image_name = imgDir(j).name;

*image =imread(strcat(file_path,image_name));*

B(:,:,j)=image;

end
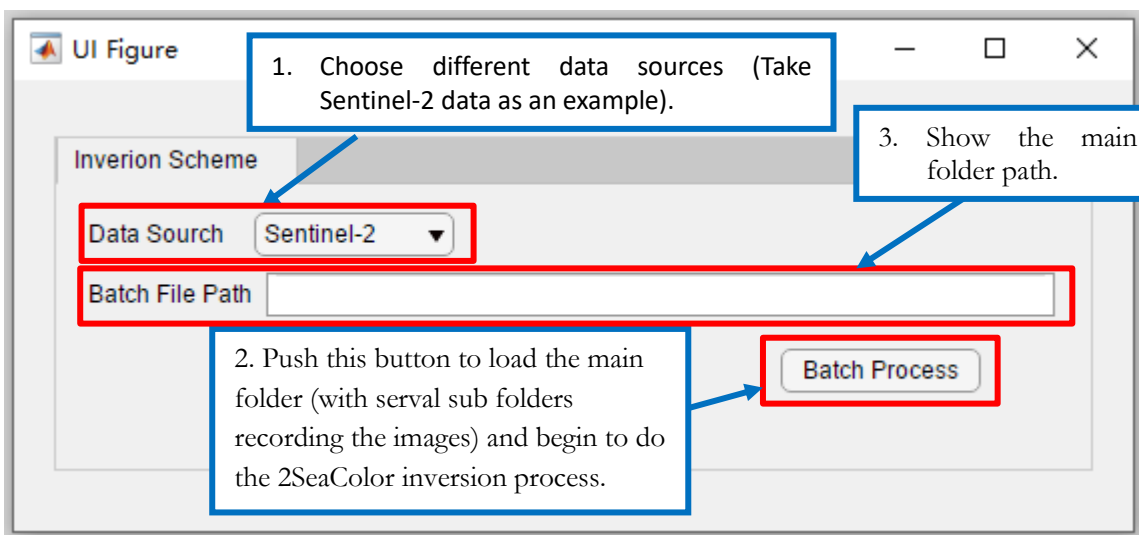
Figure 10: Interface introduction and specific steps of software operation for the batch images processing purpose.
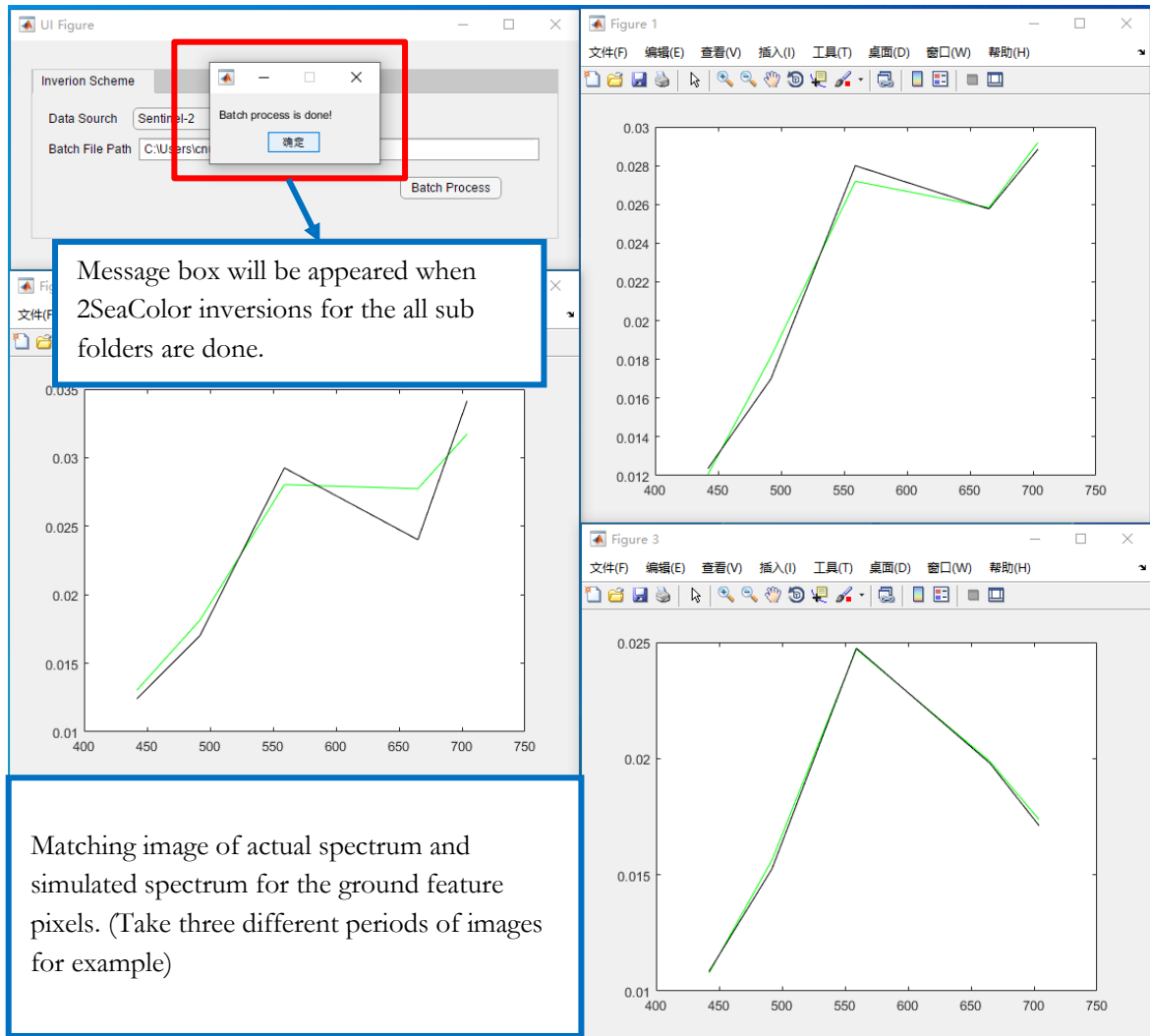
Figure 11: Procedure chart for the batch images processing when loading reflectance from different bands and doing the model inversion

4. 2SEACOLOR INVERSION SCHEME AND GEO CALIBRATION/VALIADION

This section lists the IOPs coefficients distribution in the Liao River delta and presents the SIOPs coefficients derivative process. The validation is for the comparison between measurement results and estimated results from spectrometer and satellite image reflectance, respectively.

4.1. Inherent optical properties(IOPs) distribution

The underwater light is related to the absorption and scattering processes that occur within the water column(Campbell et al., 2011). For example, water constituents, such as phytoplankton, detrital particles, and color dissolved organic matter (CDOM), are absorbed the underwater light. The absorption of these components directly determines the attenuation of light, thus determining the amount of light required for photosynthesis by plankton and benthos(Hoge & Lyon, 1996). The size of the compositional absorption coefficient is defined as inherent optical properties (IOPs), which are determined by the concentration of water constituents in the underwater body(Bricaud et al., 1995) and the presence of phytoplankton communities(Johnsen & Sakshaug, 2007). The specific inherent optical properties (SIOPs) are the water quality parameters, and their spatial variations are correlated to the underwater light. They are defined by the type and quality of absorption, also related to the phytoplankton community and the source of dissolved organic matter and particulate matter(Le et al., 2015). Obtain the values of SIOPs can help to model the underwater light fields, and they are also essential for remote sensing applications.

Absorption (a) and backscattering (b_b) coefficients are the two important factors of IOPs. They are essential for determining the light field in water, and they also perform as the link between remote sensing and concentrations of optically active water constituents(Lin et al., 2009). These two coefficients usually depend on various external factors, like wind speed, wind direction, wave height, observation incidence angle, polarization, and transmission frequency. From the Section 1.3 Literature review, there are various algorithms that have been approved that have the ability to retrieved IOPs from the apparent optical properties (AOPs). Typical properties of AOPs are the R_{rs}, and the diffuse attenuation coefficient of downwelling irradiance (K_d), are connected to the IOPs via the radiative transfer model. Thus, from the known AOPs, the a and b_b coefficients can be derived through the estimated IOPs. And further, these coefficients are the variables to get the SIOPs in the specific Liao river delta.

The first step is to inverse reflectance to IOPs at the 61 sampling locations via the 2SeaColor inversion scheme. The R_{rs} recorded from the radiometric measurement was used to do the parameterization and calculate the IOPs at the 61 samples' locations.

Take the 61 surfaces remote sensing reflectance as the samples, and the 2SeaColor inversion scheme was used to process the IOP of the Liao River delta. All of the backscattering of SPM and the absorption of the chlorophyll-a and CDOM coefficients at 440 nm. The maximum, minimum, mean values, and standard deviation of these three watercolor constituents are lists in Table 5.

Table 5:Inherent optical properties (IOPs)results(derived from 2SeaColor inversion model)

	$b_{b_{spm}}$	a_{chla}	a_{CDOM}
Maximum	0.2121	2.4868	1.9077
Minimum	0.0033	0.0016	0.4419
Mean	0.0896	0.6092	1.1045
Standard Deviation	0.0603	0.4485	0.4919

The derived concentrations of chlorophyll-a and SPM, and absorption of CDOM from these estimated IOPs were compared with available in situ measurement results from the commercial laboratory to check constancy later. Furthermore, limitations and sources of uncertainties associated with the accuracy were discussed.

4.2. GEO calibration and validation

4.2.1. Specific inherent optical properties (SIOPs) derived
In the Liao River Delta, 61 in situ data samples were divided into two groups based on even and odd data, 31 samples for retrieving the SIOPs values and the others for validation. The classification obeyed the odd-even distribution. All locations of sampling points are uniformly distributed during the calibration and validation process. Same as the Section 1.5.2 flowchart part, and the SIOPs derivation is based on the 2SeaColor inversion scheme part.

SIOPs were calculated from the GEO-Calibration. IOPs were generated from the 2SeaColor inversion model (See Table 5), and the concentrations of chlorophyll-a and SPM, and absorption of CDOM were reported from the laboratory. These two types of values were used to derive the SIOPs in the Liao River delta. In this derivation, 31 samples from the fieldwork were taken to retrieve SIOPs. The relation between SIOPs and IOPs coefficients is the mathematic relation. The relation for the chlorophyll-a is subject to quadratic functions, and relations for SPM and CDOM are linear functions.

(a)   (b)
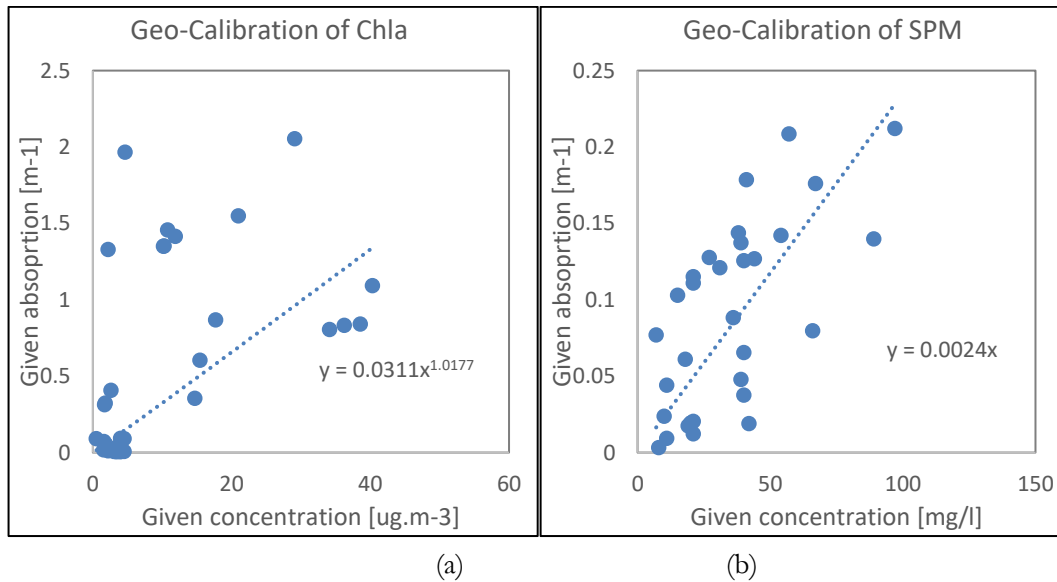
Figure 12: Specific inherent optical properties (SIOPs) derived process, GEO Calibration results of the Chl-a (a) and SPM (b) from in situ measurement concentrations and surface remote sensing reflectance.
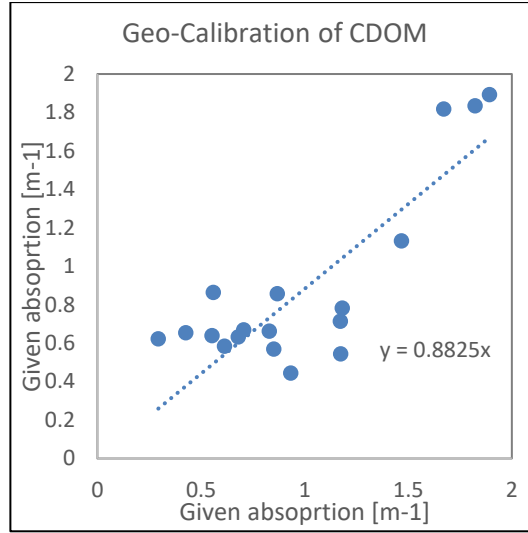
Figure 13: Specific inherent optical properties (SIOPs) derived process, GEO Calibration results of the CDOM from in situ measurement concentrations and surface remote sensing reflectance.

The results of the derived values of the SPM specific backscattering coefficient and the specific absorption coefficients of chlorophyll-a and CDOM are shown in Table 6.

Table 6: Specific inherent optical properties Derived Results

Coefficients	Derived Values	Units
a_{chla}^*	0.0311	m^2mg^{-1}
p	1.0177	-
$b_{b_{spm}}^*$	0.0024	m^2g^{-1}
k	0.8825	-

Equation $a_{CDOM}(\lambda) = a_{CDOM}(440)\exp(-s(\lambda - 440))$ from Section 3.2.2, defined k $=\exp(-s(\lambda - 440))$.

4.2.2. Geo validation

The left samples were used to do the validation. First, the concentrations and absorption for these 30 samples were estimated, based on the generated SIOPs coefficients and the corresponding mathematic relation (Section 4.2.1), and then compared the estimated result with the measured values. The correlation between the derived values and measured values was present in Fig 14 and Fig 15. In order to validate the inversion model with the fitting degree, (a) the determination coefficient R², (b) Root Mean Squared Error (RMSE) and (c) the Mean Absolute Error (MAE) were used to compare and analyze the accuracy and error of the model.

(a) The R square value shows these three estimated water constituents' values are closed to the measurement values. R² is calculated as:

$$R^2 = \left(\frac{\sum_{i=1}^{n}(X_{obs,i} - \overline{X_{obs}})(X_{model,i} - \overline{X_{model}})}{\sqrt{\sum_{i=1}^{n}(X_{obs,i} - \overline{X_{obs}})^2} \cdot \sqrt{\sum_{i=1}^{n}(X_{model,i} - \overline{X_{model}})^2}} \right)^2$$

Defined，$\overline{X_{obs}} = \frac{1}{n}\sum_{i=1}^{n} X_{obs}, \overline{X_{model}} = \frac{1}{n}\sum_{i=1}^{n} X_{model}.$

(b) Root mean square error (RMSE) is the square root of the square of the deviation between the predicted value, the measured value, and the ratio of the sample number N. RMSE is very sensitive to the reflection of the maximum or minimum error in a set of measurements, so it can well reflect the dispersion degree of a data set. The equation is the list below:

$$RMSE = \sqrt{\frac{1}{n}\sum_{i=1}^{n}(X_{obs,i} - X_{model,i})^2}$$

(c) Mean absolute deviation (MAD) is the sum of absolute difference between the actual value and the forecast divided by the number of observation. It is a summary of statistics of statistical dispersion or variability. MAD is calculated as:

$$MAD = \frac{1}{n}\sum_{i=1}^{n}|y_i - x_i|$$

The data screening is followed by the equation of relative error. Considering the relationship between data volume and modeling accuracy, 80% was selected as the screening standard.

$$\delta = |\frac{V_A - V_E}{V_E}| * 100\%$$

Where: δ is the percent error, V_A is the actual value observed, V_E is the expected error.

(a)   (b)
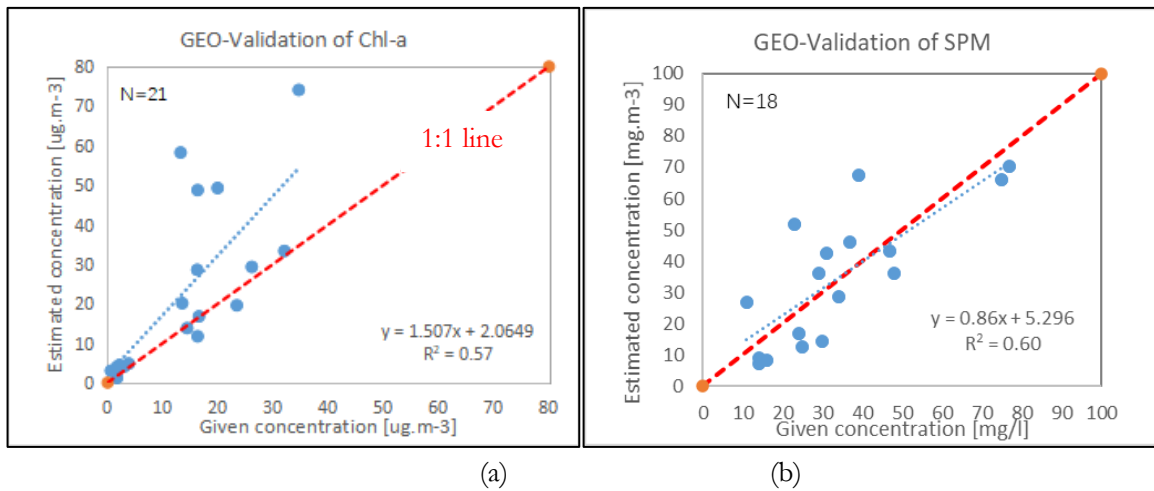
Figure 14: Scatter plot of the in situ measured Chl-a (a) and SPM (b) concentrations versus 2SeaColor model estimated Chl-a and SPM concentrations from spectrometer reflectance.
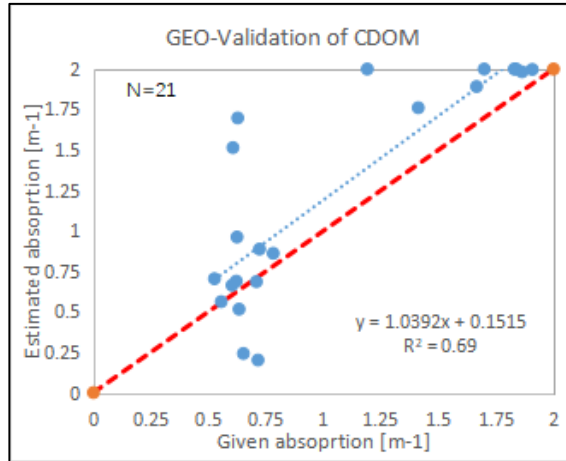
Figure 15: Scatter plot of the in situ measured CDOM absorption versus 2SeaColor model estimated CDOM absorption from spectrometer reflectance.

Table 7: Fitting mathematical indicators (Comparisons between the corresponding concentration values of model inversion values and the measured concentration values)

Constituents	R^2	RMSE	MAD
Chl-a	0.57	11.52	6.32
SPM	0.60	12.40	11.20
CDOM	0.69	0.32	0.23

From the validation results, all of these three constituents show a good inversion result. There is only a slight difference in inversion accuracy between these three, and Chlorophyll-a has the best result. The accuracy is acceptable. Therefore, the upper SIOPs coefficients were used to derive the concentrations and absorption in the Liao River delta.

4.2.3.   Satellite image estimated validation

Take the full mosaic size Sentinel-2 images on the date September 24, 2019 (same time period with the fieldwork) as a case.

(a)   (b)
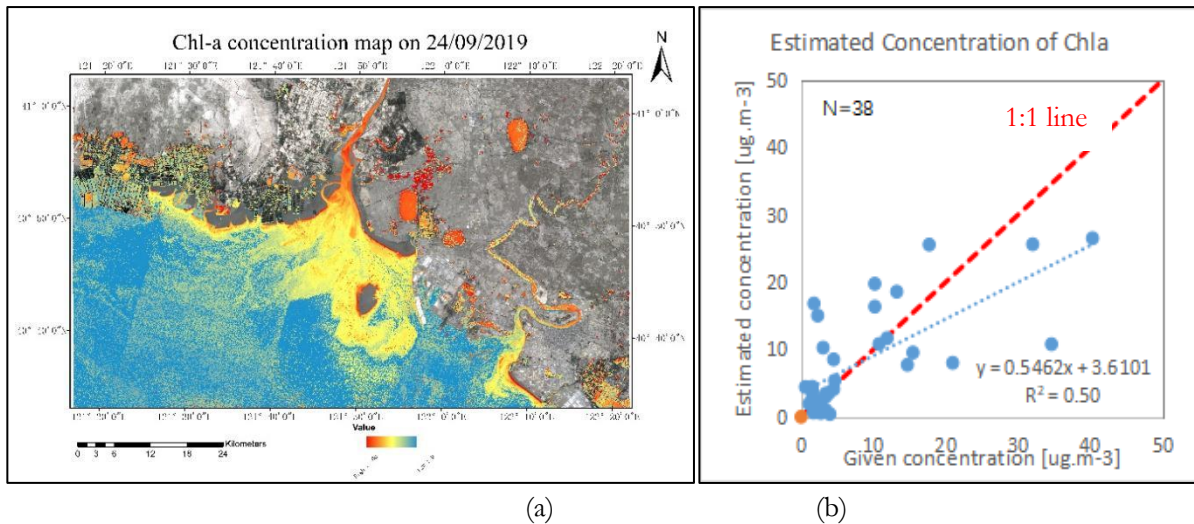
Figure 16: (a) Estimated Chl-a concentrations from 2SeaColor model[Unit: ug/m³];(b)Scatter plot of the validation results of in situ measured Chl-a concentrations versus 2SeaColor model estimated Chl-a concentrations from Sentinel-2 MSI images. (Black pixels are the river background of the satellite image.)
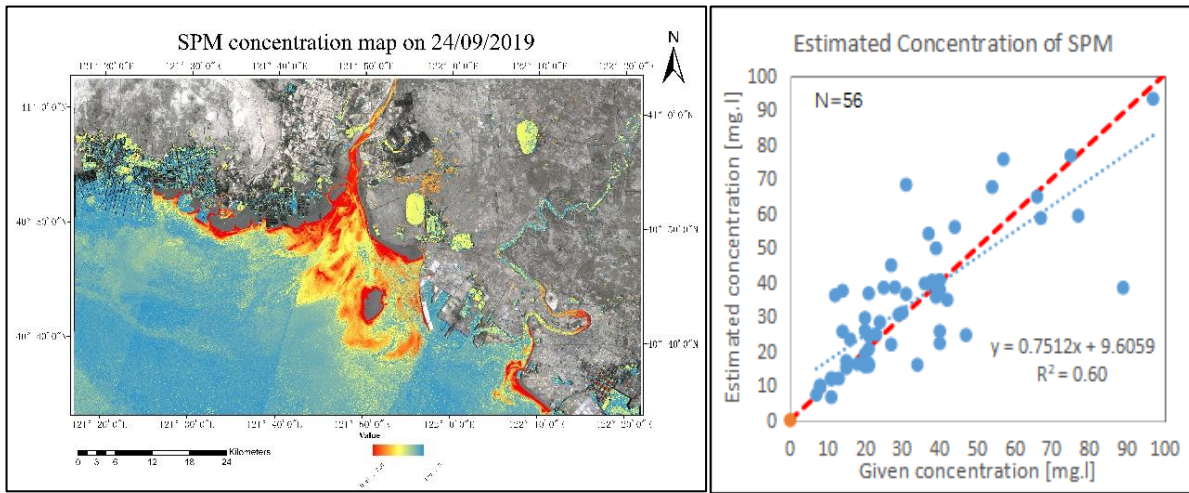
(a)   (b)

Figure 17: (a) Estimated SPM concentrations from 2SeaColor model[Unit: mg/l];(b)Scatter plot of the validation results of in situ measured SPM concentrations versus 2SeaColor model estimated SPM concentrations from Sentinel-2 MSI images.
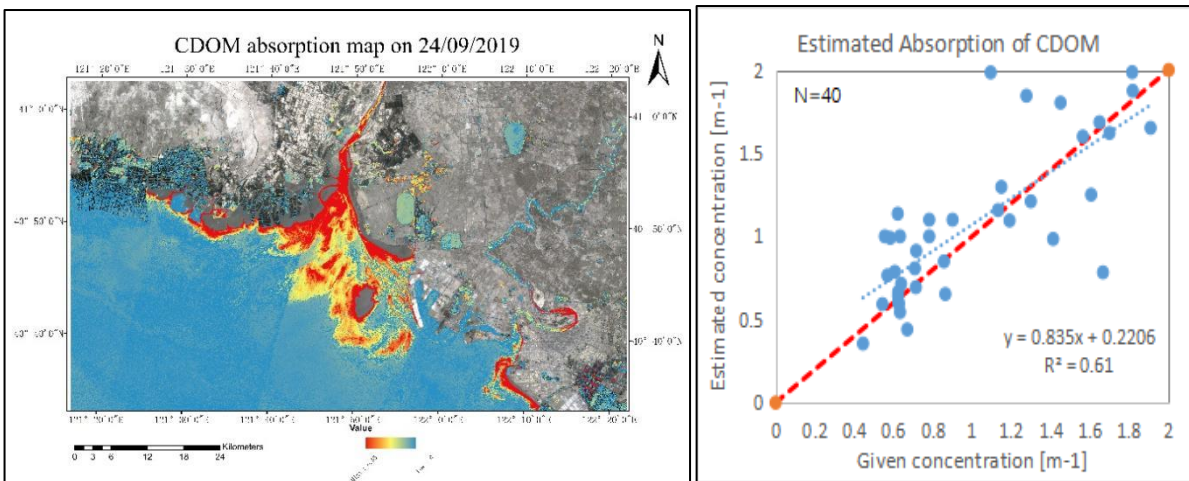
(a)   (b)

Figure 18: (a) Estimated CDOM absorption from 2SeaColor model[Unit: m⁻¹];(b)Scatter plot of the validation results of in situ measured CDOM absorption versus 2SeaColor model estimated CDOM absorption from Sentinel-2 MSI images.

Table 8: Fitting mathematical indicators (Comparisons between the corresponding concentration values of the same derived period Sentinel-2 images inversion values and the measured concentration values)

Constituents	R^2	RMSE	MAD
Chl-a	0.50	13.85	8.60
SPM	0.60	13.52	8.70
CDOM	0.61	0.31	0.22

The concentrations and absorption of the sampling locations were export from the estimated maps. Scatter plots above show the comparison of the satellite estimated results with the measurement results. Although the same time period was controlled on this process, the differences are obvious. Sentinel-2 MSI images are more sensitive for the CDOM and SPM inversion, and its ability for Chlorophyll-a has not had advantages. However, considered the experiment operability and spatial scale three water constituents distribution in the Liao River delta, the overall inversion results are significant, which is suitable for the concentration inversion of water at other times.

Generated water constituents concentrations (WCCs) map of chlorophyll-a in Fig 16 (a) shows the range is from 0 to 50 ug/m³, and high values are concentrated upon the area near the build-up region. The majority values are between 10 to 30 ug/m³, and they are located at the estuary of the Shuangtaizi River. The chlorophyll-a concentration at the Shuangtaizi River is slightly higher than the Daliao River. The concentration map shows the concentration of chlorophyll-a in the area near land and shoal is obviously higher than that in the middle of the river. Human has a strong influence at the Shuangtaizi River. So that means the outflow of the Shuangtaizi River and the Daliao River were evidently influenced by human activities. And the concentration of chlorophyll-a is affected by human activities and shoals.

Fig 17 (a) is the WCC map of SPM. The range is between 0 and 300 mg/l. High concentration appeared in the Shuangtaizi River, and the deposition of suspended solids of the Daliao River was much better. The majority values are between 100 to 220 mg/l, most of them located at the central position of the Shuangtaizi River, near the west bank of the shoal. And the concentration of SPM in the Shuangtaizi river is obviously higher than it in the Daliao River, and the average concentrations are most likely changed from 150 to 30 mg/l. The higher concentration of SPM is concentrated in the area around the shore water body and shoal. SPM is related to the concentration of colloidal materials and clay minerals. And sediment transport is another reason for SPM concentration.

The absorption of CDOM was below 6.55 m^{-1} in Fig 18 (a), high absorption spread to the Bohai Sea. The majority value is 2 m^{-1}, which appeared at the central position of the Shuangtaizi River, near the west bank of the shoal. The area around the shore water body and shoal also show a higher concentration of CDOM than the central river areas and pelagic waters. The Shuangtaizi river also shows significantly higher CDOM absorption than the Daliao River. But different from SPM spatial variation, at the bend of the Daliao River, there is a clear absorption region, and its absorption is about 5 m^{-1}. The absorption rate of CDOM is closely related to the photochemical process, such as organic degradation. High absorption represents more degradation of organic matter.

5.   TEMPORAL AND SPATIAL VARIATION

This section shows the three water constituents' spatial and temporal variation from 2016 to 2020. Concentration plots and absorption maps are arranged in chronological order. Sentinel-2 MSI images automatically defined the non-water pixels on their images, and some of the "NoData" values have appeared in this area. Checking the "Bohai sea bay tide table", those area appearances were mainly because the satellite transit time, close to 3 am, coincides with the time of low tide. And the sea height is below 0.26m at the low tide, so Sentinel-2 images are defined as shoals in the open water. But the tide conditions change daily, therefore at the same time as the satellite's transit, other times images come flooding in, and the satellite detects and identifies the entire ocean. The processing of atmospheric correction, ACOLITE tools, was only base on the water pixels from satellite images. Therefore, except for the "NoData" pixels from the raw reflectance images, the concentrations were generated via the 2SeaColor model. In the WCCs maps, the blank white area is the famous Gaizhou shoal in the Liao river delta, and other missing data areas were filled with the blue background color. The using Sentinel-2 MSI images were listed in Table 9.

Table 9: Sentinel-2 MSI images data collection table

Year	Water Level	Date	Satellite Image Information
2016	Wet	8.22	S2A_MSIL1C_20160822T023552_N0204_R089_T51TUF_20160822T024021
			S2A_MSIL1C_20160822T023552_N0204_R089_T51TVF_20160822T024021
	Normal	11.23	S2A_MSIL1C_20161123T025022_N0204_R132_T51TUF_20161123T025214
			S2A_MSIL1C_20161123T025022_N0204_R132_T51TVF_20161123T025214
2017	Wet	9.29	S2A_MSIL1C_20170929T024541_N0205_R132_T51TUF_20170929T025548
			S2A_MSIL1C_20170929T024541_N0205_R132_T51TVF_20170929T025548
	Normal	11.20	S2B_MSIL1C_20171120T023959_N0206_R089_T51TUF_20171120T100326
			S2B_MSIL1C_20171120T023959_N0206_R089_T51TVF_20171120T100326
2018	Wet	8.25	S2A_MSIL1C_20180825T024551_N0206_R132_T51TUF_20180825T054557
			S2A_MSIL1C_20180825T024551_N0206_R132_T51TVF_20180825T054557
	Normal	10.24	S2A_MSIL1C_20181024T024751_N0206_R132_T51TUF_20181024T073519
			S2A_MSIL1C_20181024T024751_N0206_R132_T51TVF_20181024T073519
2019	Wet	9.24	S2B_MSIL1C_20190924T024549_N0208_R132_T51TUF_20190924T053202
			S2B_MSIL1C_20190924T024549_N0208_R132_T51TVF_20190924T053202
	Normal	10.29	S2A_MSIL1C_20191029T024831_N0208_R132_T51TUF_20191029T055056
			S2A_MSIL1C_20191029T024831_N0208_R132_T51TVF_20191029T055056
2020	Wet	9.25	S2B_MSIL1C_20200925T023549_N0209_R089_T51TUF_20200925T044821
			S2B_MSIL1C_20200925T023549_N0209_R089_T51TVF_20200925T044821
	Normal	11.27	S2B_MSIL1C_20201127T025039_N0209_R132_T51TUF_20201127T040852
			S2B_MSIL1C_20201127T025039_N0209_R132_T51TVF_20201127T040852
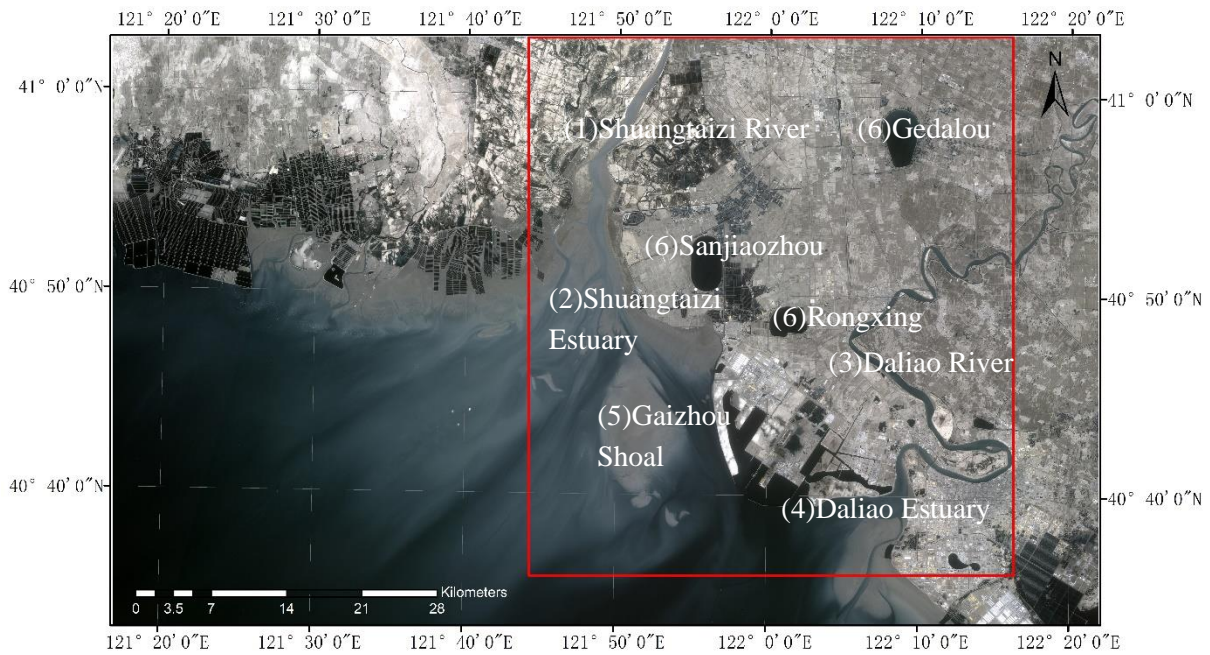
Figure 19: Mathematical analysis of partition statistical chart.

For the mathematical analysis, based on the characteristics of the landscape, the research area has been divided into six parts, see Figure 18: (1) Shuangtaizi River, (2) Shuangtaizi estuary, (3) Daliao River, (4) Daliao estuary, (5) Gaizhou Shoal surrounding, and (6)Inland reservoirs (Including Sanjiaozhou reservoir, Gedalou reservoir, and Rongxing reservoir). These landscape types are classified into open water and inland reservoirs. There are sixty samples in all, and every ten samples were selected from each part. All of the samples were evenly distributed around these five parts. The concentration and absorption data were extracted from these samples, and their average values were used for analysis.

5.1. Chlorophyll-a (Chl-a) variation

5.1.1. Five-year inversion maps of Chl-a

(a)2016.08.22

(b)2016.11.23

(c) 2017.09.29

(d)2017.11.20

(e)2018.08.25

(f)2018.11.18

(g)2019.09.24

(h)2019.10.29

(i)2020.09.25

(k)2020.11.27

Value
High : 100
Low : 0

0 50 100   200 Kilometers
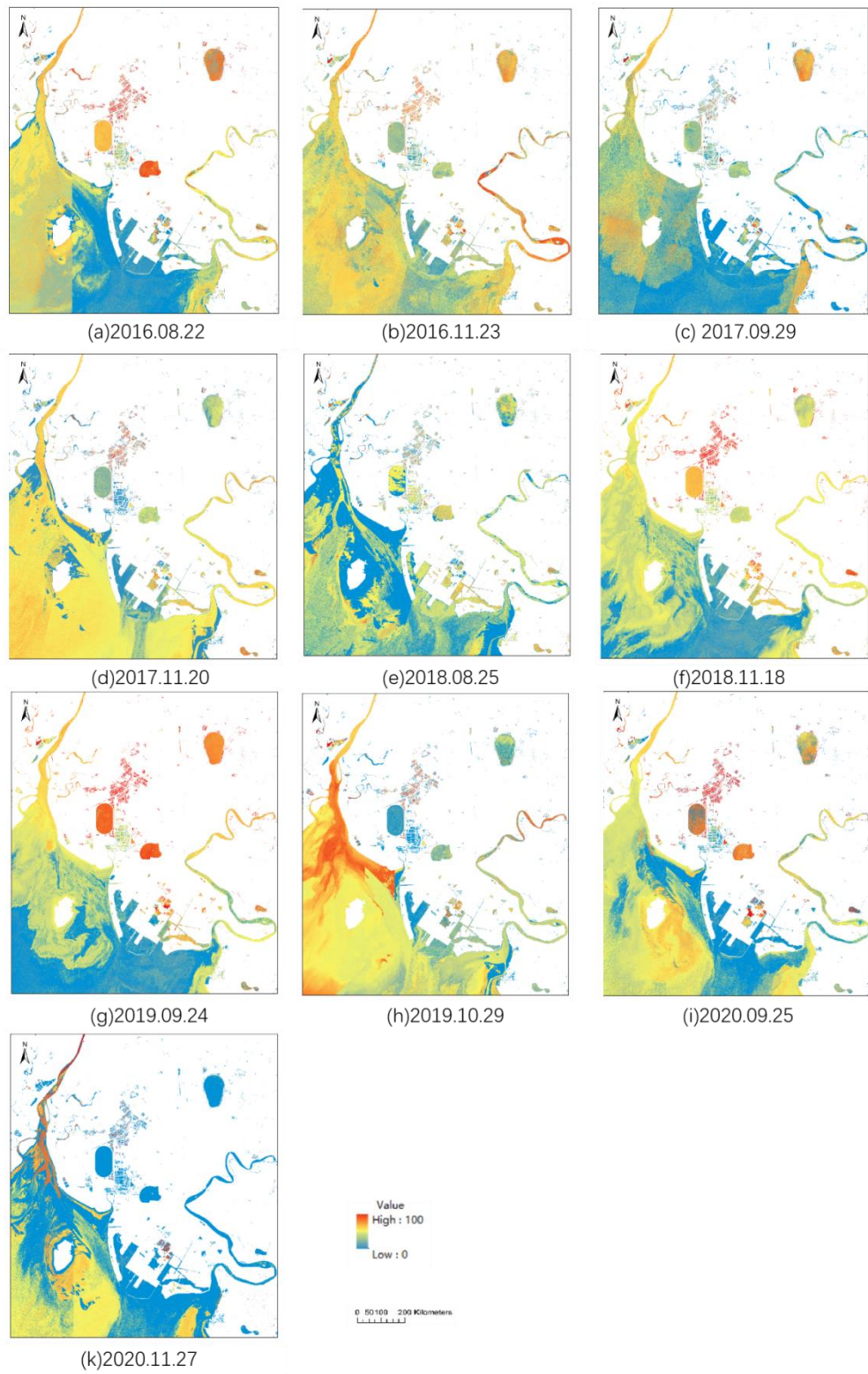
Figure 20: Temporal and spatial variation of chlorophyll-a concentration, from 2016 to 2020 UNIT[ug/m³].

Through the combined analysis of inversion maps from 2016 to 2020 and mathematical statistics, the conclusions are as follows: (1) For the annual variation of chlorophyll-a concentration in the Liao River Delta, the difference is not significant. And the average concentration range of the estuary is between 20 ug/m³ and 40 ug/m³, and very few areas are above 100 ug/m³. (2) The inversion results of five years show that the seasonal concentration cycle of chlorophyll-a is relatively stable for the high water level period and normal water level period. In terms of spatial variation, there is a decreasing trend from rivers to estuary and to Bohai sea. (3) High concentration areas are located at the bend of the Shuangtaizi river and Daliao River, near the land. Basically, the concentration is relatively large, often presenting a mild or moderate eutrophication state, which may be related to the discharge of domestic sewage, aquaculture, and frequent human activities. The shallow lake water along the coast is rich in nutrients, leading to the vigorous growth of algae. There is also a high concentration of chlorophyll-a in the waters near Gaizhou shoal. This is because the islands and reefs provide places for phytoplankton to attach to and places for fish and other marine organisms to survive and reproduce(Wu et al., 2016), forming a virtuous cycle of the Marine ecosystem food chain. (4) The increase of chlorophyll-a concentration is the result of the inversion of algal aggregation. Appropriate temperature, wind direction, and stable water conditions are conducive to its reproduction. In the Liao River region, there is not much difference in surface temperature between these two months in the wet season and the normal season. However, in the wet season, the Liao River delta is prone to heavy rain, with high intensity, high frequency, fast current gathering, and strong wind, which makes the water exchange speed fast, and is not conducive to reproduction of algae. Compared with the inland reservoirs, the water discharge speed of the open water is fast. Therefore, the chlorophyll-a concentration is slightly higher in the normal season in the open water area, but lower at the inland reservoirs.

5.1.2.   Regional variation analysis of Chl-a
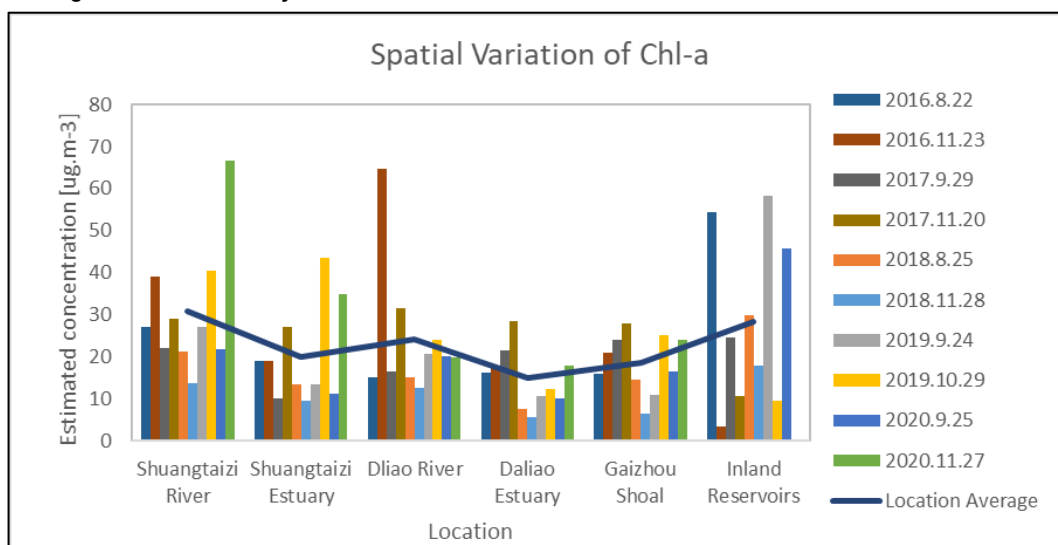
Figure 21:Inversion value of chlorophyll-a concentration based on location distribution.

Figure 21 lists the variation of chlorophyll-a concentration from 2016 to 2020. It obviously shows the variation difference. The maximum value of the chlorophyll-a concentration is up to 100 ug/m³. From the

samples, Shuangtaizi River shows the highest concentration concentrated, and the average in these five years is 30.81 ug/m³. Reservoirs and Daliao River are in second and third place, with a value of 28.26 ug/m³ and 24.10 ug/m³. The concentration around Shuangtaizi estuary and Gaizhou shoal are close to 20.16 ug/m³. Daliao estuary has the lowest value, about 14.90 ug/m³.

The concentration of Chla-a is related to the sea surface temperature (SST), especially for the variation of inland reservoirs. Higher temperature leads to higher concentration in the reservoirs, and it explains the wet period has a Chl-a concentrated than the normal period (Xu & Fan, 2018). For the open water, SST gradually increases from coastal to offshore areas and from summer to winter. In terms of spatial correlation, there is a negative correlation between Chl-a concentration and SST, and the correlation degree is different in different sea areas. There is a strong correlation between the concentration of Chl-a in the open sea, so it leads to a decreasing trend from the estuary to the open sea. But in near-land coastal areas, due to the influence of human production and living, the correlation between seawater temperature and chlorophyll concentration is not obvious(Shan et al., n.d.).

5.1.3. Temporal variation analysis of Chl-a
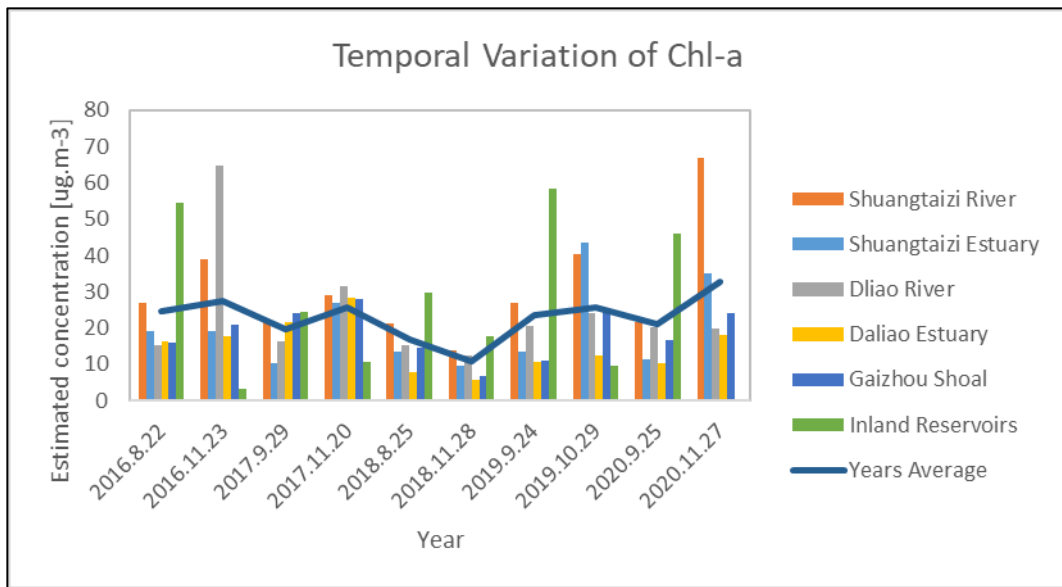
Figure 22： Inversion value of chlorophyll-a concentration based on time distribution.

Figure 22 shows the seasonal and annual differences. These five years have a smooth change, and it means the variation of chlorophyll-a is not significant. It also shows high values in the normal season and low values in the wet season for the average concentration.
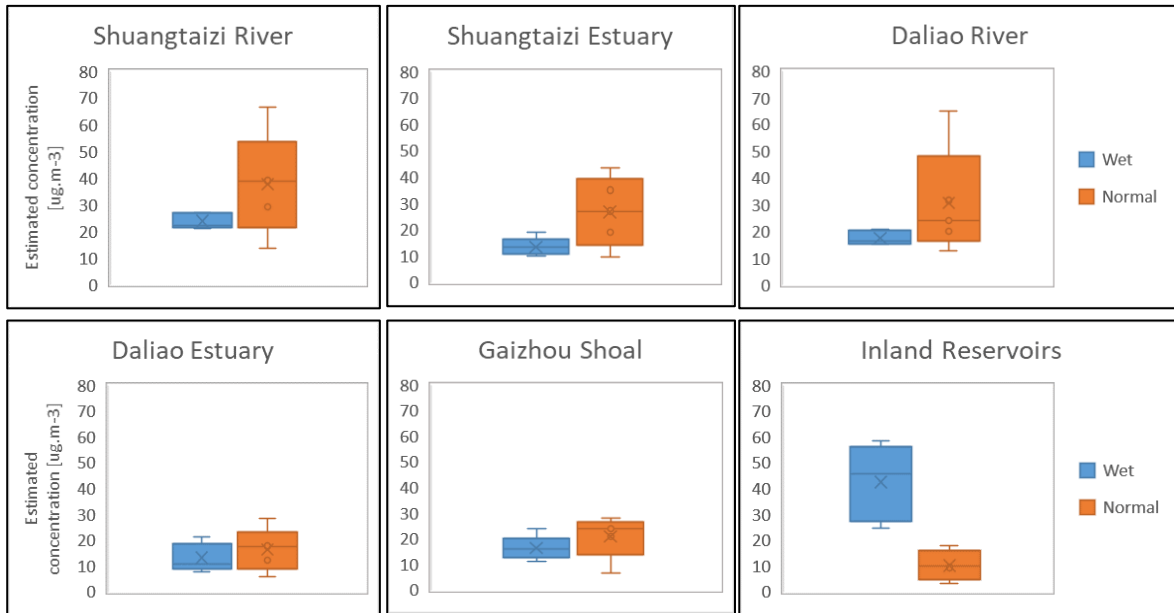
Figure 23:Side-by-side boxplots of Chl-a concentration seasonal changes in six locations.

Boxplots can effectively show the data discretization and look for indicators of nonnormal or unusual data. (1) Compared with the seasonal difference in the inland reservoirs, the concentration data of chlorophyll-a in the other five locations were scattered in the normal season and concentrated in the wet season, and in general, the wet season has a stable condition in these five years, but normal season varies greatly. (2) The data of inland reservoirs had an opposite dispersion. (3) In the meantime, the dispersion degree of river data in the normal period was higher than that of estuarine data and shoal data. It means the Shuangtaizi river and Daliao river had an obvious concentration change of chlorophyll-a in the normal season. (4) The distribution of the data represents the probability concentration range. This eliminates errors due to random sampling. The results show that the wet season samples from Shuangtaizi Estuary, Daliao river, and Gaizhou shoal were overestimated on actual average data. And the normal season samples from Shuangtaizi Estuary and Gaizhou shoal were underestimated the regional average.

5.1.4. Inland reservoirs variation of Chl-a
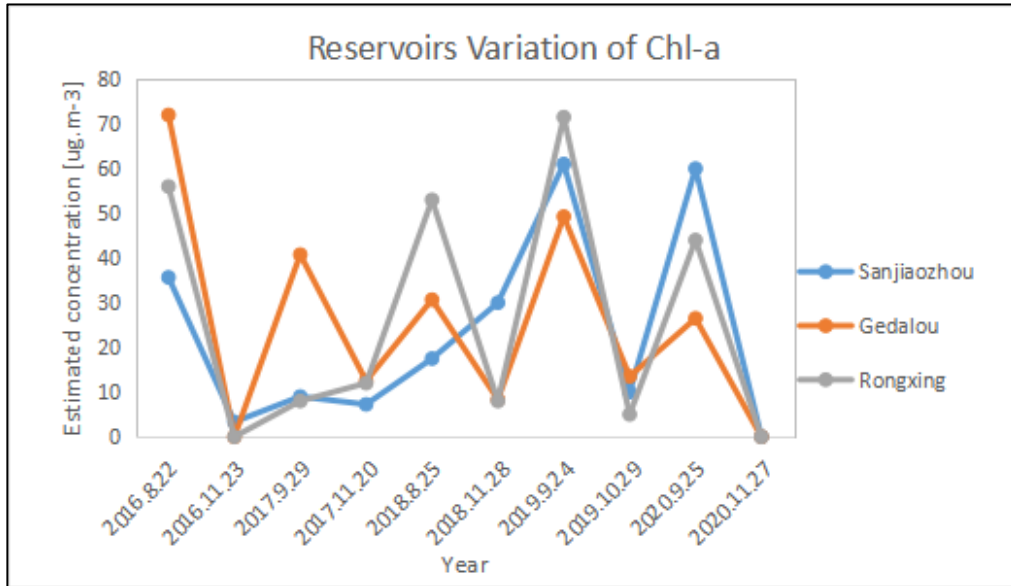
Figure 24: Inland reservoirs variation of Chl-a.

Seasonal changes of inland reservoirs variation of chlorophyll-a are different with open water. The concentration in the wet season is higher than the normal season. In these three reservoirs, the Gedalou reservoir and the Rongxing reservoir were average at 31.93 ug/m³, and the Sanjiaozhou reservoir was a little lower, about 25.97 ug/m³. Also, the Sanjiaozhou reservoir shows a noticeable fluctuation from November 2017. But the Gedalou reservoir fluctuated steadily. The variation of the Rongxing reservoir is mainly because lots of farmlands on the east bank have been transformed into fishponds. The discharge of domestic sewage(Dong Dandan, 2020), aquaculture, and frequent human activities acted together to raise Chl-a concentration.

5.2. Non-algal suspended particulate matter (SPM) variation

5.2.1. Five-year inversion maps of SPM
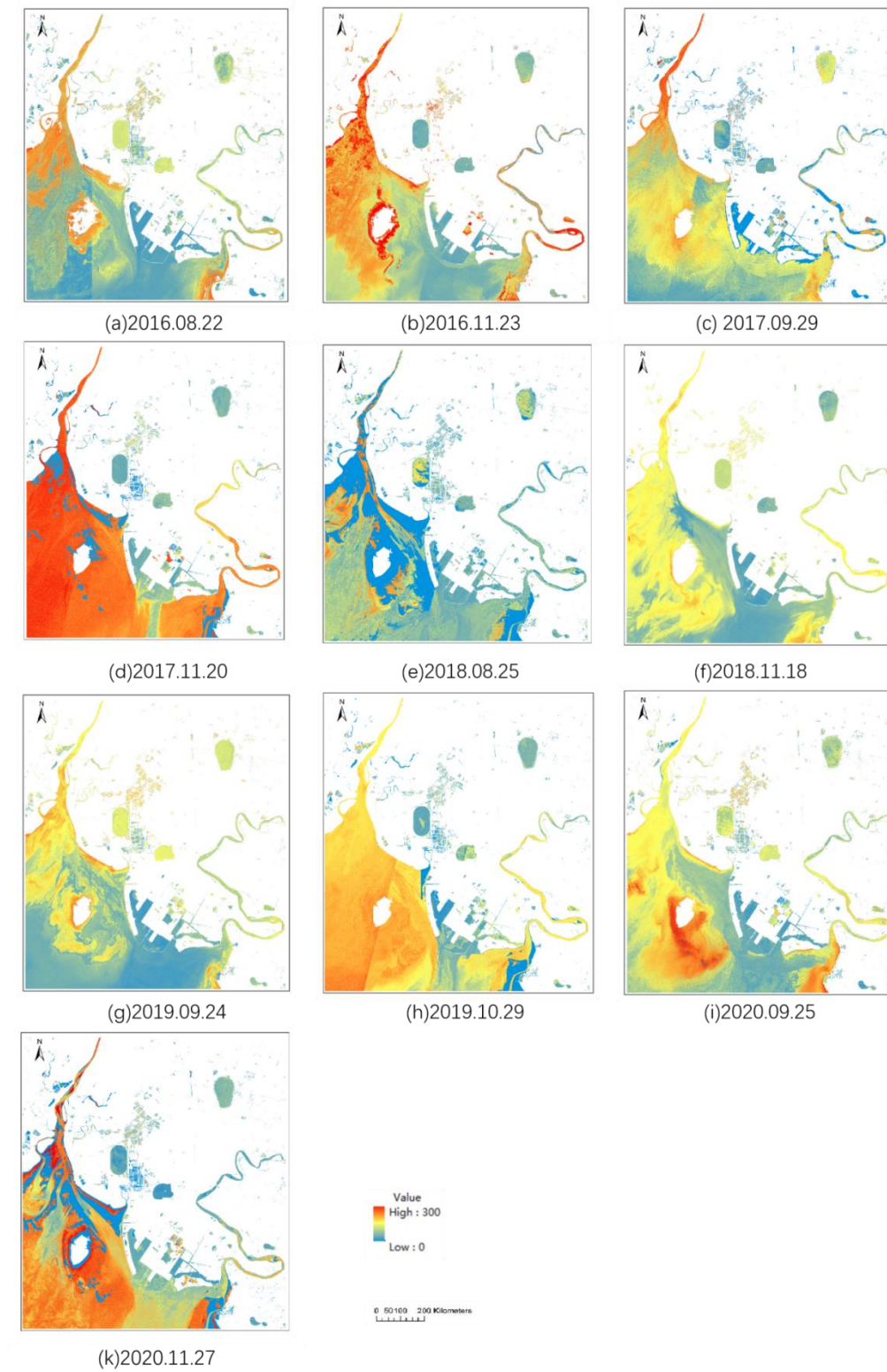
Figure 25: Temporal and spatial variation of SPM concentration, from 2016 to 2020 UNIT[mg/l].

The variation of SPM is as follows: (1) SPM shows regular seasonal changes in the Liao River delta. For most of these five years, the concentration in the normal season is higher than it in the wet season. The maximum annual mean concentration is about 175 mg/l in November. (2) SPM concentration shows a decreasing trend from north to south, and high concentration near shore and low concentration far shore. (3) Shuangtaizi River has more suspension aggregates than the Daliao River and estuary. Due to the shallow water depth, strong hydrodynamic force, and the input of debris material (sediment) from the main saliferous rivers(Gao Chen et al., 2019), the suspended matter content in the nearshore sea area is obviously higher than that in the open sea area. (4) Open water area has higher SPM concentration than inland reservoirs. The main reason is that the Liao River estuary area has developed the aquaculture industry and also accepts the shipping work in the area. The disturbance of the past hull makes the suspended solids hover in the estuary area. But for the inland reservoirs are mainly used for irrigation and drinking by human activities, and the water dynamic is relatively slight.

5.2.2. Regional variation analysis of SPM
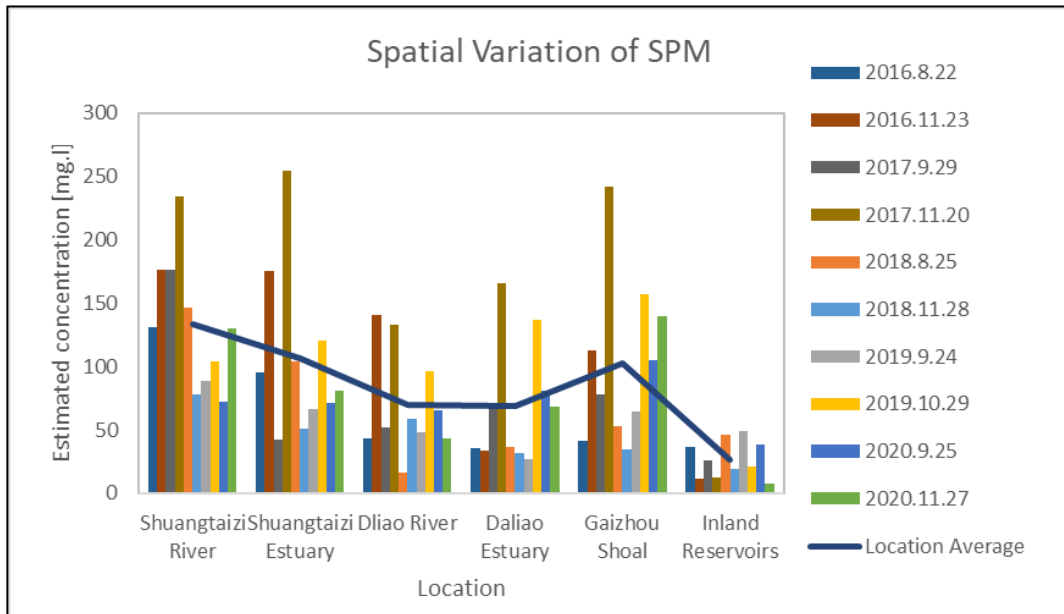
Figure 26: Inversion value of SPM concentration based on location distribution.

In these five years, SPM has an obvious seasonal change, but not an annual. The Shuangtaizi River has the highest concentration of SPM at 133.60 mg/l. They were followed by the Shuangtaizi estuary and Gaizhou shoal, 106.02 mg/l and 102.82 mg/l, respectively. The SPM concentration at Daliao River and estuary are below 100 mg/l, and the range of these two areas is between 68 to 70 mg/l. The SPM concentration in the reservoirs is significantly lower than the river, a value of 26.74 mg/l.

5.2.3. Temporal variation analysis of SPM

Figure 27:Inversion value of SPM concentration based on time distribution.
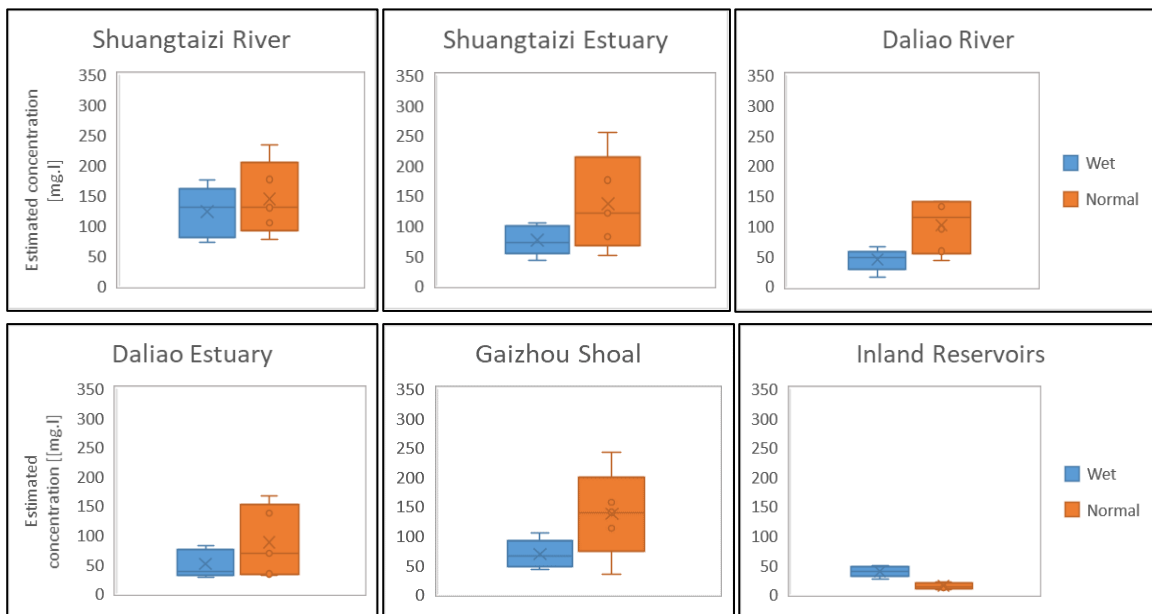
Figure 28: Side-by-side boxplots of SPM concentration seasonal changes in six locations.

(1) The data dispersion of SPM was more serious than that of Chl-a, and the concentration data in the normal season also showed a scattered condition, except the location of the inland reservoir. (2) The data of inland reservoirs were stable and concentrated, so the sampled data can well show the variation of SPM. (3) The SPM concentration of the Daliao river was also relatively steady during these five years, but the other four locations in the open water had a great change, especially in the normal season. (4) The sampling mean concentration still shows an error relative to the actual mean concentration. The seasonal sampling average data in the Daliao river was underestimated and the Daliao estuary was overestimated the actual condition.

5.2.4. Inland reservoirs variation of SPM
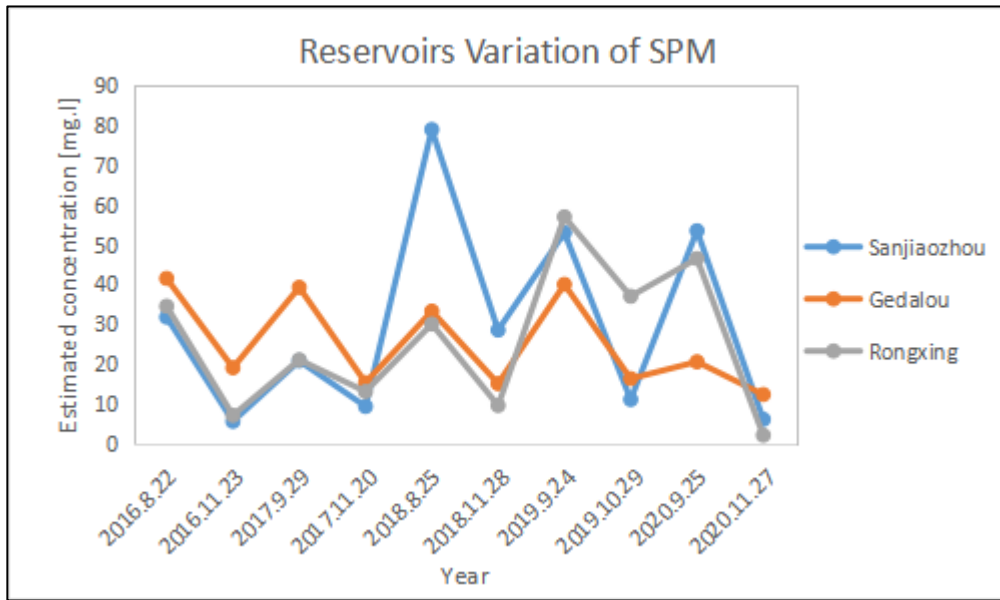
Figure 29: Inland reservoirs variation of SPM.

Seasonal changes in SPM are stable in these five years. All of these three reservoirs show higher values in the wet season, but low values in the normal season. Sanjiaozhou reservoir has the highest concentration at 29.83 mg/l, followed by the Rongxing reservoir about 25.75 mg/l, and the lowest average concentration appears in the Gedalou reservoir at 25.23 mg/l. A particularly high value appeared at the Sanjiaozhou reservoir in August 2018. Before this date, the concentration in this reservoir was lower than the others. It represents an SPM gathering and leads to a high SPM condition in the following years. The source of the SPM is likely to be surrounding agricultural land. Checking from the Google maps, there were lots of fishponds dried up and used for farmland from 2018.

5.3. Colored dissolved organic matter (CDOM) variation

5.3.1. Five-year inversion maps of CDOM

(a)2016.08.22

(b)2016.11.23

(c) 2017.09.29

(d)2017.11.20

(e)2018.08.25

(f)2018.11.18

(g)2019.09.24

(h)2019.10.29

(i)2020.09.25

(k)2020.11.27
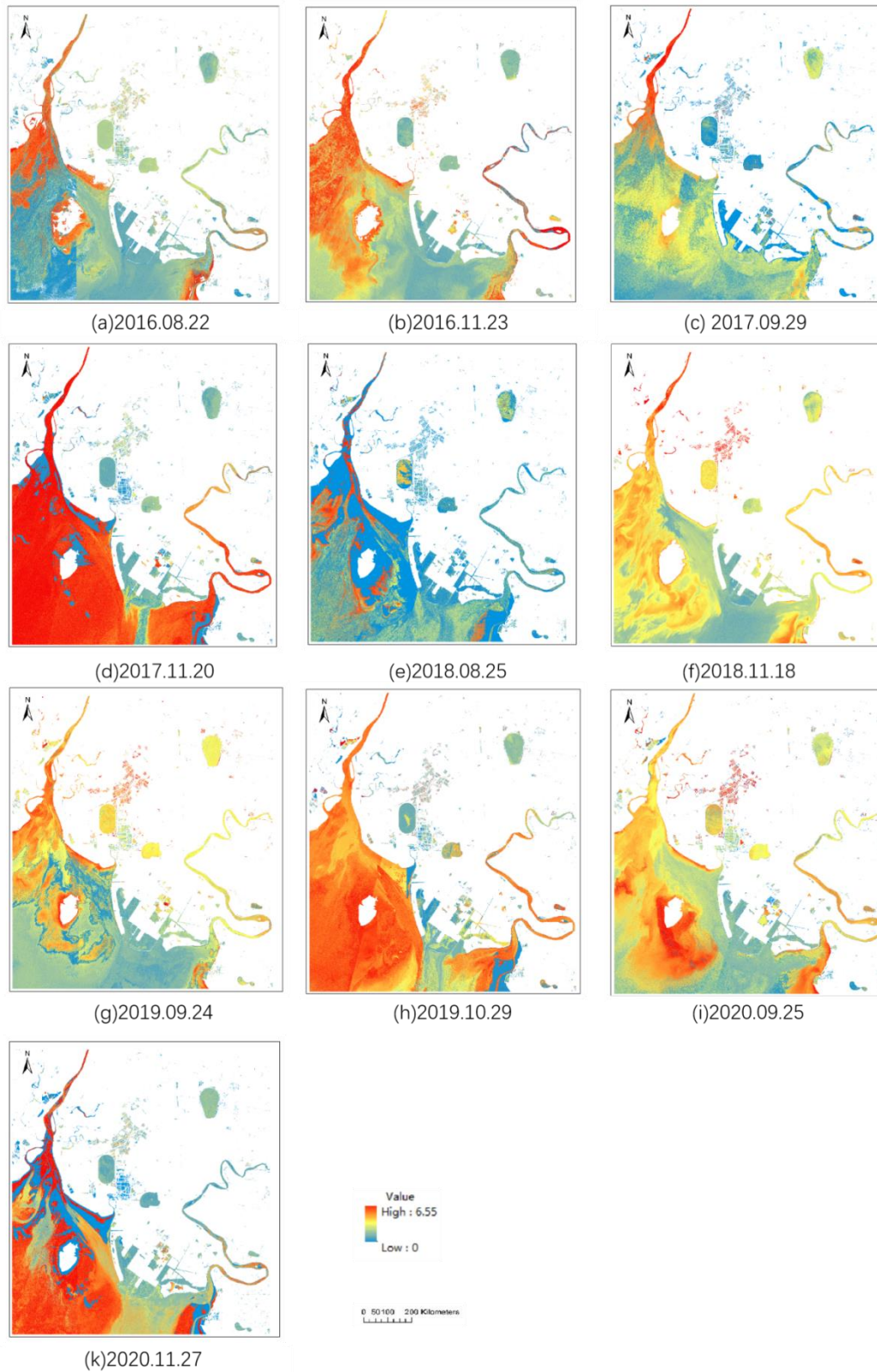
Figure30: Temporal and spatial variation of CDOM absorption, from 2016 to 2020 UNIT[m-1].

According to the above information, the following conclusions can be drawn: (1) In these five years, CDOM absorption in the normal season is higher than it in the wet season in 2017, 2019, and 2020. But in the years 2016 and 2018, the absorption differences are slight. Wet season average absorption is about 2.5 m^{-1} in the Liao River delta, and the normal season is about 5 m^{-1}. The variation is close to the SPM variation. (2) It shows a gradually decreasing trend of CDOM in the range of rivers to estuaries and to the sea area. The spatial variation can be inferred that the main source of CDOM in the Liao River delta is land-based input. (3) There is a lot of sewage from villages living near the Shuangtaizi River, and human settlements near the Daliao River, and these tributaries are long and narrow, resulting in a high CDOM in these two rivers. Around the Gaizhou shoal, because of the slow flow of water and easy settlement of nutrients, the growth of phytoplankton is accelerated(Zheng Shuxian et al., 2019), which increases the concentration of CDOM. (4)CDOM absorption at the inland reservoirs is obviously lower than the open water. The first reason is that, water discharge in open water is frequent, a large number of dissolved organic matter adsorption in the particulate matter, resulting in the increase of CDOM in the water. Another reason is that the open water region gets more rain than the inland area(Liang et al., 2020). Due to the increased precipitation, a large amount of runoff carries nutrients into rivers and estuaries, and the temperature in the normal season is suitable for the phytoplankton growth and extinction alternate, thus promoting the increase of CDOM content.

5.3.2.   Regional variation analysis of CDOM
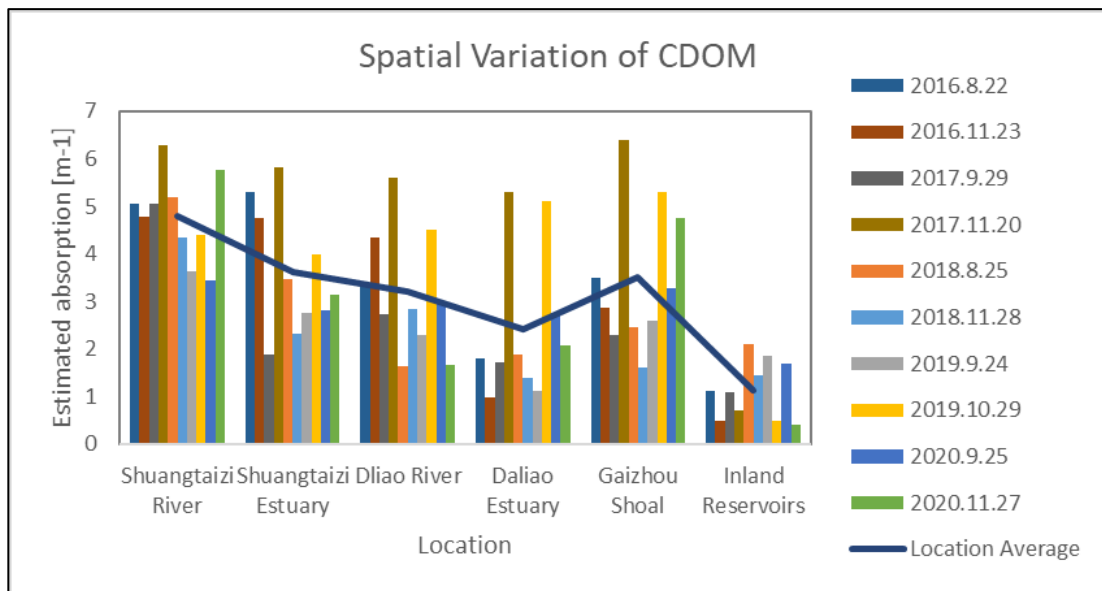
Figure 30: Inversion value of CDOM absorption based on location distribution.

The variation of average CDOM absorption in these five years is similar to SPM. The highest absorption values appear in the Shuangtaizi River, about 4.80 m^{-1}. Shuangtaizi estuary has an absorption at 3.63 m^{-1}, and Gaizhou shoal is about 3.51 m^{-1}. Different from SPM variation, the Daliao River is higher than the Daliao estuary, 3.20 m^{-1}, and 2.41 m^{-1}, respectively. The lowest absorption appears in the reservoirs, value of 1.14 m^{-1}.

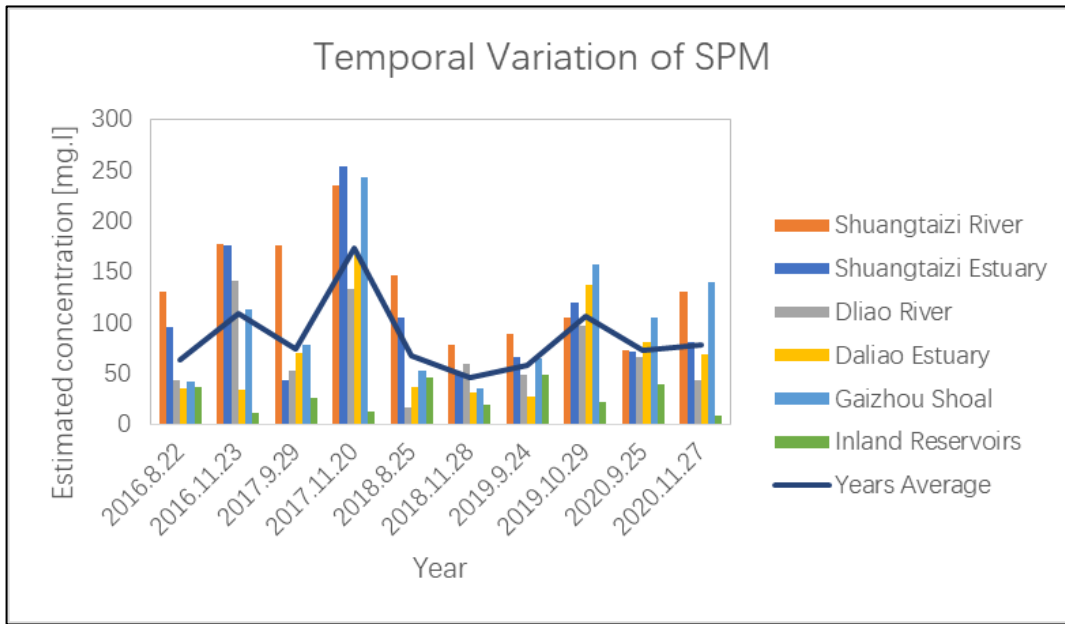### 5.3.3. Temporal variation analysis of CDOM
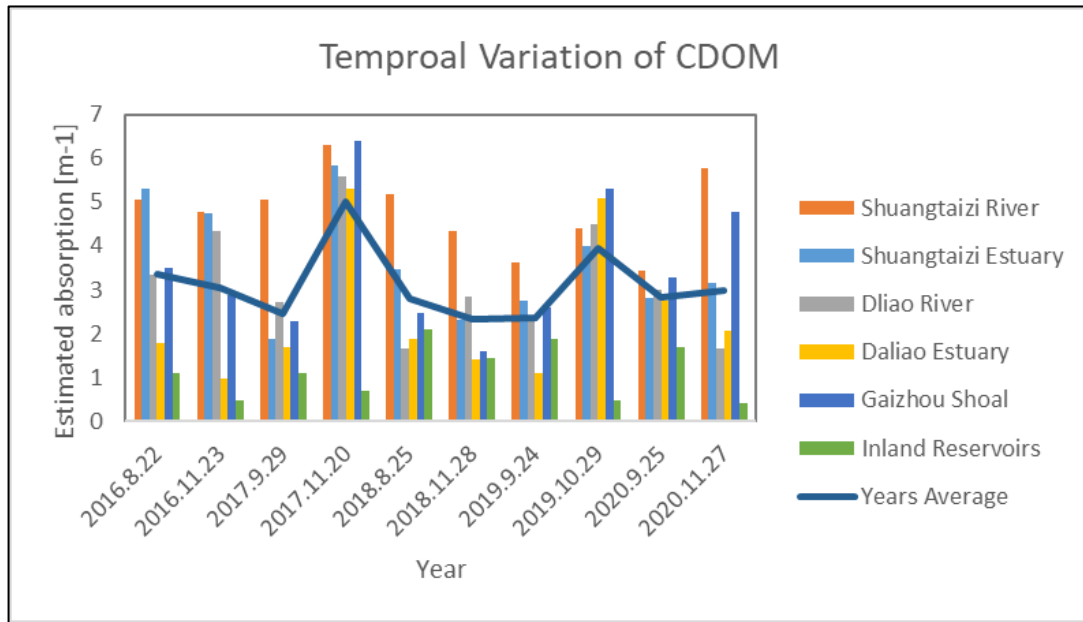
Figure 31: Inversion value of CDOM concentration based on time distribution
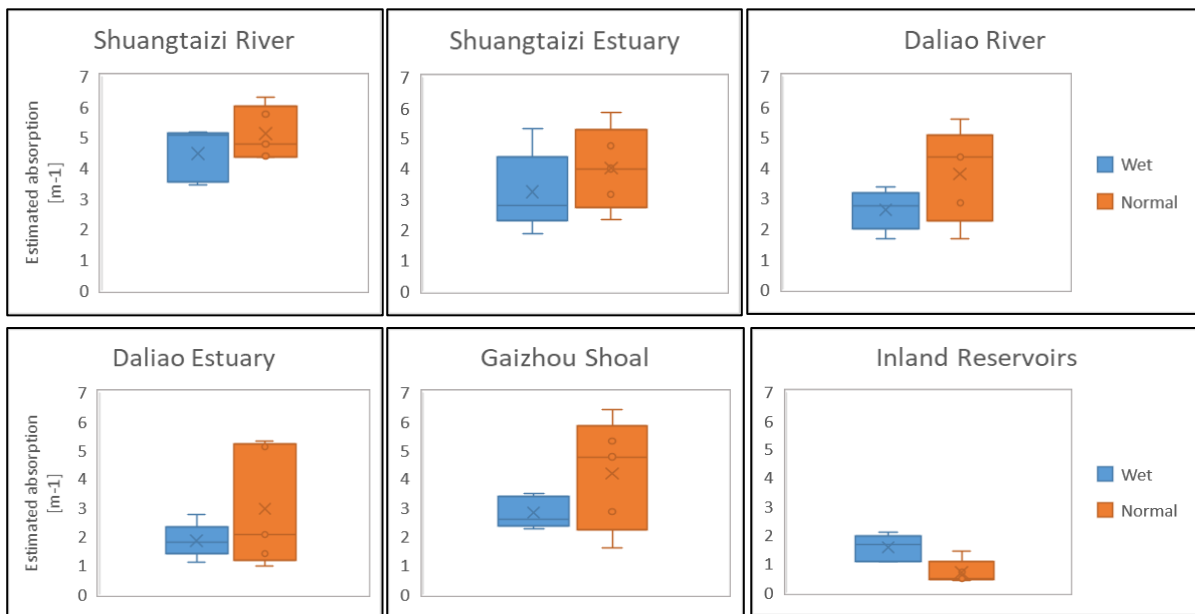
Figure 32: Side-by-side boxplots of CDOM concentration seasonal changes in six locations.

(1) The data dispersion of CDOM was more evident than the other two. It means CDOM variation in these five years has a serious temporal variation. (2) The data of inland reservoirs were also stable and concentrated, similar to the variation of SPM. (3) The change of the normal period was still greater than that of the wet period. Especially for the Daliao Estuary, the absorption range was changed from 1 m^{-1} to 7 m^{-1}. (4) Most of the sampling points uniformly show the normal distribution of data. Skewed data appeared in Shuangtaizi river, Shuangtaizi estuary, Daiao estuary and Gaizhou shoal. In the wet season, the average sampling condition of Shuangtaizi estuary and Gaizhou shoal was very likely overestimated the

actual average absorption, and Shuangtaizi river was the opposite. In the normal season, the sampling absorption of the Daliao estuary showed a positive skew distribution.

5.3.4. Inland reservoirs variation of CDOM
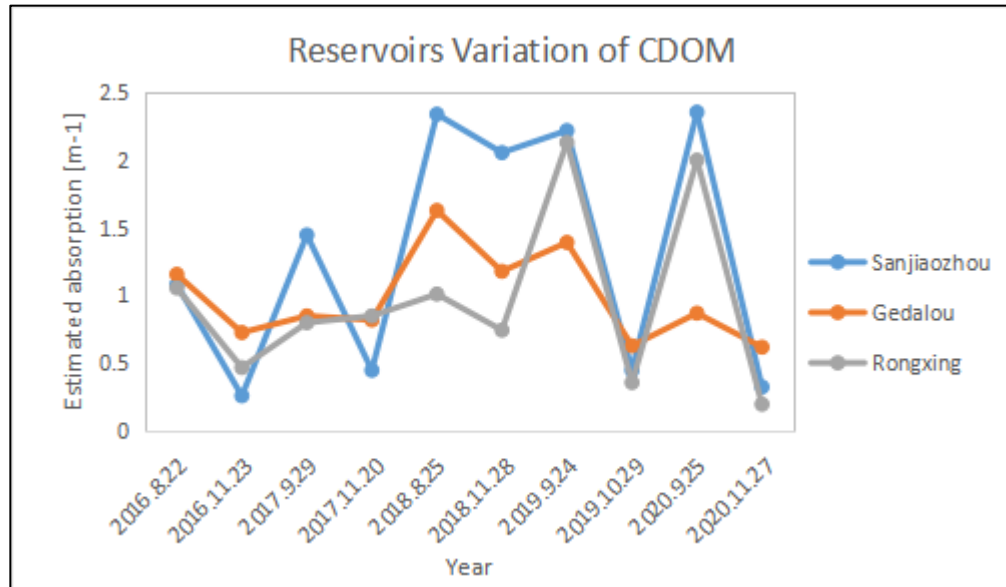
Figure 33: Inland reservoirs variation of CDOM.

The maximum-to-minimum sort result of CDOM absorption is the same with SPM. Highest average values at the Sanjiaozhou reservoir about 1.44 m^{-1}, and the lowest values at the Gedalou reservoir around 0.99 m^{-1}. To a great extent, the CDOM source came from the suspended solids. The SPM carried the CDOM and stored it in the reservoirs. Different from the open water, water discharge was slow here, and high absorption condition was maintained after 2018.

5.4. Impact factors and pollution sources analysis

5.4.1. Fine-scale water dynamic superiority

Twenty meters resolution inversion results give strong evidence for the analysis of the water dynamic changes and reveal the pollution sources. (1) Chlorophyll-a is more influenced by human activities. In this region, there are lots of small tributaries connected to the Shuangtaizi river and Daliao river. The end of these small tributaries is linked to the farmland and residential district. All of the sewages from aquaculture, life and industry and agriculture were a guide to the mainstream. The concentration map in Figure 20 shows the condition of the high value of these tributaries. (2) SPM is an essential basis for the study of sediment transport and geomorphic evolution, which can help predict sediment carrying capacity and play an important role in the study of sediment transport laws in coastal waters. The variation of SPM can not only explore the situation of seawater pollution, but also further trace the flow path of pollutants and the direction of pollutants in seawater. It can represent the movement path and change the law of pollutants in seawater, so as to provide technical support for seawater pollution control. (3) CDOM is the product of phytoplankton degradation, and the fine-scale absorption map shows where these organisms reside in the river, such as the west bank of the Shuangtaizi river and the east bank and the bend of the

Daliao river, and the area near Gaizhou shoal. Fine-scale maps clearly show the difference in CDOM absorption.

5.4.2. External drivers

The water quality of the estuarine is well known affected by the aggravation of various pollutants, such as aquaculture, life and industry and agriculture, which enter the lake every year with the groundwater. Besides, some of the meteorological events can affect the WCCs condition. (1) Heavy rainfall events bring a lot of exogenous substances to the estuaries, which change the nutrient concentration of the river and show signs of accelerated eutrophication. (2) Strong winds will drive land-based pollutants to estuaries and closer seas, resulting in an increase of WCCs. At the same time, strong winds will drive the continuous fluctuation of water flow, so that suspended substances and nutrients cannot settle to the bottom of the river, affecting the underground light field. (3) The seasonal cycle determines the WCCs in the sea surface temperature and cloudy atmospheric conditions. For the Liao River delta, excluding the influence of high temperature in summer and river icing in winter, the temperature in autumn is more suitable for the reproduction of phytoplankton and meanwhile provides a source of nutrients for aquatic organisms. With the increase of chlorophyll-a content, a large amount of CDOM is generated by degradation. Also, due to the cloudy air in autumn, the atmospheric correction cannot completely exclude the influence of haze, resulting in the high reflectivity of the reverse performance.

5.4.3. Fishery industry pollution and potential risks

There are two obvious breeding industry places in the study area, the first one is located on the west bank of Shuangtaizi River, where the river enters the estuary. And the second place of fish ponds is near the inland reservoirs. Analyzed these two regional WCCs of the fish ponds, chlorophyll-a concentration in the wet season is around 20 ug/m³, and 45 ug/m³ in the normal season. The average SPM concentration of this area is a maximum to 300 mg/m³ in both wet and normal seasons. The CDOM absorption is around 6 m⁻¹ in the wet and normal season. These data are all above the mean value (see Table 10) in the area where they belong, and prove the fishery industry increase the WCCs in the Liao River delta. Especially for the SPM concentration and CDOM absorption, significant differences in WCCs distribution can also be seen in Figure 25 and Figure 30.

Table 10: Five years average concentration of WCCs.

Location	Shuangtaizi River	Shuangtaizi Estuary	Daliao River	Daliao Estuary	Gaizhou Shoal	Inland reservoirs
Chl-a[ug/m³]	32.26	19.29	24.47	17.06	19.23	27.86
SPM[mg/l]	149.26	113.22	73.31	80.61	112.84	27.74
CDOM[m⁻¹]	4.98	3.85	3.39	2.64	3.59	1.22
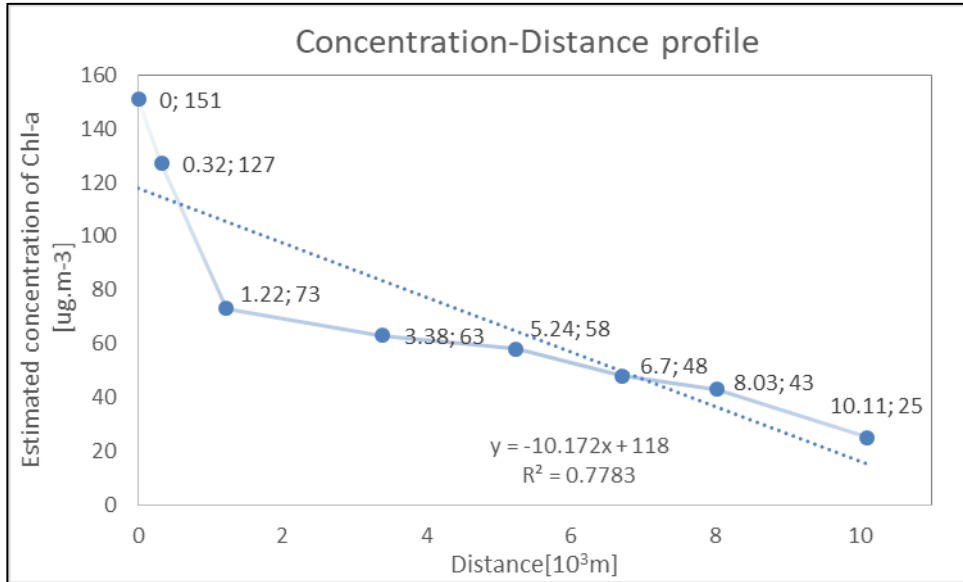
Figure 34: Relevance plot between Chl-a concentration and fishpond distance (Take the inversion map from September 24, 2019, as a case).

Processed the distance and Chlorophyll-a concentration relation, it has an obvious negative correlation. The concentration of chlorophyll-a varies with the distance from the fishponds, and the farther the distance, the lower the concentration. This figure is strong evidence to show the correlation between Chlorophyll-a pollution and fishponds location. The same study was used for SPM and CDOM, but no correlation was found. The results showed that chlorophyll-a pollution was more serious in the three water constituents, but no noticeable effect was found in the other two elements.

Chlorophyll-a is a basic measure of ocean productivity and is used to characterize phytoplankton abundance. The suspended matter pollution in natural culture areas mainly comes from domestic sewage, rainfall, and industrial wastewater. And fish waste can also form suspended solids to some extent. CDOM adsorption exists on suspended solids, and it represents the degree of eutrophication to some extent.

These concentrations have proved suitable for the fish industry. But the suspended matter pollution needs to be taken seriously, especially for the west bank of the Shuangtaizi river. The excess suspended matter will affect the fish respiratory system, consumption of dissolved oxygen, reduce the benefit of farming. The abnormal proliferation of phytoplankton in the water (especially harmful algae such as cyanobacteria) consumes a large amount of oxygen in the water, making the water quality worse. Therefore, from the perspective of aquaculture and water pollution, the water quality pollution on Shuangtaizi estuary needs human attention.

6. CONCLUSIONS AND RECOMMENDATIONS

6.1. Research summary

Affected by the turbidity of the water body, the water constituents concentrations(WCCs) inversion in Case Ⅱ water has seen little progress(Chami & Robilliard, 2002). In order to solve the current situation, that the Liao River Estuary is a typical representative, which is not conducive to the inversion of water quality concentration, this study uses a new semi-analytical model--2SeaColor radiative transfer model to carry out the three water constituents concentrations, including Chlorophyll-a (Chl-a), Non-algal suspended particulate matter (SPM) and Colored dissolved organic matter (CDOM). In this study, firstly, the atmospheric correction method, ACOLITE, was used to obtain the highly accurate remote sensing reflectance from the satellite images. And ACOLITE correction method based on the DSF model was proved to have a higher result, and applied in the following processing. Secondly, five years WCCs inversion study was conducted on the Sentinel-2 MSI L1C data from 2016 to 2020. Thirdly, the spatial and temporal variation of three constituents were analyzed base on the inversion maps and mathematic diagrams. Pollution sources and influencing factors were also mentioned in the analysis part. The main findings of this article are as follows:

(1)The 2SeaColor model inversion interfaces were constructed in the Liao River delta area, using Matlab App Designer as a tool, which realized the simultaneous inversion of single and multiple images and optimized the operability of the model.

(2)The SIOPs coefficients of the Liao River delta were simulated from 61 in situ water quality data, sampled in September 2019. The absorption coefficient a_{chla}^* of Chl-a, the power parameter p, the backscattering coefficient of SPM $b_{b\,spm}^*$, and the absorption coefficient weight k of CDOM was parameterized on 0.0311 m^2mg^{-1}, 1.0177, 0.0024 m^2g^{-1}, and 0.8825, respectively. Based on these coefficients, the WCCs inversion model in the Liao River delta was constructed, and R2 values of these three constituents are 0.57, 0.60, and 0.69, respectively, which confirms that the above parameters are suitable for the inversion of the concentration of the three elements of watercolor in the Liao River delta. 2SeaColor model fundamentally explains the relationship between the reflectance from water and the IOPs, confirming that the model can still be used even when the water body is highly turbid and ensure high inversion accuracy. To a great extent, the problem of WCCs inversion in the Case Ⅱ water is solved within this model.

(3)Atmospheric correction was performed on the Sentinel-2 MSI satellite images of ten scenic spots during the wet and normal water level periods from 2016 to 2020, to obtain the R_{rs}. The water quality monitoring in the Liao River delta region was completed for five years. At the same time, the accuracy of the model was verified with remote sensing image data synchronized with the satellite and the ground, and the R2 values of these three constituents were simulated to be 0.50, 0.60, and 0.61, respectively. Sentinel-2 MSI images are more sensitive for the CDOM and SPM inversion. But considering the Sentinel-2 spatial-temporal resolution, it is believed that the model is suitable for WCCs inversion with Sentinel-2 as the background data, and it has the ability to do the long time series inversion.

(4)Based on the spatial and temporal variation analysis of WCCs in these past five years, it was confirmed that the concentration of the three constituents in this region presents a spatial distribution characteristic of high concentration near shore and low concentration far shore, and gradually decreasing from north to south. The results show that the WCCs has little inter-annual variation and great seasonal variation during the five years. It was also analyzed that the outer sea and inland reservoirs present opposite seasonal changes. It was concluded that the concentration in the normal water period is higher than that in the wet period for the open water area. According to the characteristics of geographical location, the space-time variability of six sub-regions are analyzed, and the characteristics of WCCs in different regions are listed as followed:

Chl-a: For the annual variation of chlorophyll-a concentration in the Liao River Delta, the difference is not significant. Algal aggregation is the main reason for the increase of chlorophyll-a concentration. Comparison of annual average concentrations in different regions: Shuangtaizi River＞Reservoirs＞Daliao River＞Shuangtaizi River Estuary＞Gaizhou Shoal＞Daliao River Estuary. And, Gedalou reservoir＞Rongxing reservoir＞Sanjiaozhou reservoir.

SPM: SPM has a strong seasonal variation. It is concluded that the concentration in the normal water period is higher than that in the wet period, and the influencing factors are mainly because of the strong hydrodynamic force and disturbance of the past hull. Comparison of annual average concentrations in different regions: Shuangtaizi River＞Shuangtaizi River Estuary＞Gaizhou Shoal＞Daliao River Estuary＞Daliao River＞Reservoirs. And, Sanjiaozhou reservoir＞Rongxing reservoir＞Gedalou reservoir.

CDOM: CDOM variation is close to the SPM, because of a large number of dissolved organic matter adsorption in the particulate matter and active in the river. And the main source of CDOM in the Liao River delta is land-based input. Comparison of annual average concentrations in different regions: Shuangtaizi River＞Shuangtaizi River Estuary＞Gaizhou Shoal＞Daliao River＞Daliao River Estuary＞Reservoirs. And, Sanjiaozhou reservoir＞Rongxing reservoir＞Gedalou reservoir.

(5) According to the different sensitivity of inland reservoir and open sea area Chl-a to SST, the increasing and decreasing trend analysis is carried out, and the reasons for the different seasonal changes in the wet water period and the normal water period are explained. At the same time, a profile shows the negative correlation between Chl-a concentrations and distance from the fishponds, and it is concluded that Chl-a in the Liao River delta is greatly affected by the discharge of aquaculture and wastewater. SPM and CDOM variations don't show a correlation, while SPM and CDOM are affected by the water exchange rate from different water level periods, and SPM carries CDOM and hovers in the water body, resulting in similar spatial and temporal changes of the two. Besides, the current WCCs are used to analyze the environmental suitability for the survival of fish, analyze the risk brought by the current situation of water quality to the nearby aquaculture industry, and emphasize the negative impact of high SPM concentration on the local aquaculture fishery on the west bank of Shuangtaizi River.

(6) Research questions and answers:

Q1: What is the usage of Sentinel 2 MSI images in the process of retrieving WCCs?

A1: Sentinel-2 satellite images provide remote sensing reflectance, which can be used to inverse IOPs, combined with SIOPs to estimated WCCs. Sentinel-2 image provides several spectral bands for the IOPs inversion.

Q2:   What Specific Inherent Optical Properties (SIOPs) parameters need to be used in order to retrieve accurate estimates for the concentrations and absorption?

A2:   The absorption coefficient a^*_{chla} of chlorophyll-a(Chl-a) and the power parameter p, the backscattering coefficient of suspended matter (SPM) bb^*_{spm} , and the absorption coefficient weight k of colored soluble organic matter (CDOM).

Q3:   What is the accuracy of the 2SeaColor model retrieval WCCs compared with the sampled data?

A3: R^2

Chl-a: 0.57   SPM: 0.60   CDOM: 0.69

Q4:   What is the accuracy of the 2SeaColor model retrieval WCCs from the satellite image reflectance?

A4: R^2

Chl-a: 0.50   SPM: 0.60   CDOM: 0.61

Q5:   What are the spatial and temporal variations of WCCs in the Liao River delta?

A5:   WCCs have little inter-annual variation and great seasonal variation during these five years. High concentration near shore and low concentration far shore, and gradually decreasing from north to south. Shuangtaizi River had the highest concentrations of all of the three constituents in the six analyzed zones.

Q6:   How do the small-scale features reveal the water dynamic?

A6:   20 meters resolution results provide more concentration details for this research. For example, in the research, the correlation between the Chl-a concentration and the distance from fishponds was presented. When using the initial 60 meters resolution maps, this area was not inverted.

Q7:   How does the water level during the normal periods and wet periods influence the concentrations and absorption of the water constituents?

A7:   Open ocean water and inland reservoirs present opposite seasonal changes. It was concluded that the concentration in the normal water period is higher than that in the wet period for the open water area. But inland reservoirs have higher concentrations in the wet period.

6.2.   Scientific significance

(1) Previous SIOPs from the Bohai sea are verified not suitable for this research, and the estimated SIOPs for the Liao river delta are listed in this research. It provides more accurate parameters for others to study the water quality in this area.

(2) Multiple distribution maps of Chl-a and SPM concentrations and CDOM absorption covering the Liao River delta are used to show the temporal and spatial changes visually. The results can help to explain the terrestrial input pollution and propose relevant remediation suggestions.

(3) 20-meter resolutions water quality maps can present small features WCCs difference. For instance, the correlation analysis between Chl-a concentrations and distance from fishponds is based on the fine-scale results. These maps are evidence to find the source region of pollutants. And high-resolution retrieval maps can show more regional differences of the WCCs based on the sentinel-2 remote sensing reflectance.

(4) The retrieved data and the measured data can be analyzed to prove the universality of the 2SeaColor model in the Liao River delta and the Bohai sea.

6.3.   Recommendations

The derived IOPs and SIOPs have supported the ability to inverse WCCs in the Liao River delta. The research results indicate that the 2SeaColor model inversion model established in this study is more suitable for the inversion of the WCCs in the Case Ⅱ water body of the Liao River delta, and can provide a reference for the regional inversion in other Case Ⅱ water bodies and sea areas in China. This research also proves 2SeaColor model has a strong ability to apply to the Bohai Sea region.

6.4.   Limitations

In this research, due to the limitation of sampling conditions in the Liao River delta, the water sample collection is not completely synchronized with the image time, which affects the accuracy of the inversion model to some extent. At the same time, limited by the time and ability of researchers, the research process and results of this paper still need to be further improved and verified, mainly in the following aspects:

(1) The accuracy of the model needs to be precise. The concentration of water constituents is affected by various factors. The using 2SeaColor model also considers some metrology factors, like wind speed and sea surface temperature, but the fieldwork lacks these data. These data gaps can be overcome in the next field sampling, and the model inversion results will become better.

(2) The concentration maps based on Sentinel-2 MSI images have many blank pixels, result in water region pixels deficient, especially in the summer and winter seasons. It was automatically defined to the non-water pixels by Sentinel-2 images. None of the atmospheric correction processing methods, like ACOLITE and C2RCC, can extract reflectance from these pixels.

(3) The using spatial resolutions in this research are mentioned in two types, 60m for the SIOPs validation and 20m for the WCCs variation analysis. The small-scale resolution shows better performance on water dynamic changes in the same time period. But due to the time limitation, the comparison of the inverse dynamic differences between these two resolutions needs to be completed in future work.

LIST OF REFERENCES

Ambarwulan, W., Salama, M. S., Mannaerts, C. M., & Verhoef, W. (2011). Estimating specific inherent optical properties of tropical coastal waters using bio - optical model inversion and in situ measurements : case of the Berau estuary, East Kalimantan, Indonesia. *Hydrobiologia*, *658*(11), 197–211. https://doi.org/10.1007/S10750-010-0473-

Arabi, B., Salama, M. S., Pitarch, J., & Verhoef, W. (2020). Integration of in-situ and multi-sensor satellite observations for long-term water quality monitoring in coastal areas. *Remote Sensing of Environment*, *239*, 111632. https://doi.org/10.1016/j.rse.2020.111632

Arabi, B., Salama, M. S., Wernand, M. R., & Verhoef, W. (2018). Remote sensing of water constituent concentrations using time series of in-situ hyperspectral measurements in the Wadden Sea. *Remote Sensing of Environment*, *216*, 154–170. https://doi.org/10.1016/j.rse.2018.06.040

Arabi, B., Salama, M., Wernand, M., & Verhoef, W. (2016). MOD2SEA: A Coupled Atmosphere-Hydro-Optical Model for the Retrieval of Chlorophyll-a from Remote Sensing Observations in Complex Turbid Waters. *Remote Sensing*, *8*(9), 722. https://doi.org/10.3390/rs8090722

Beck, R., Zhan, S., Liu, H., Tong, S., Yang, B., Xu, M., Ye, Z., Huang, Y., Shu, S., Wu, Q., Wang, S., Berling, K., Murray, A., Emery, E., Reif, M., Harwood, J., Young, J., Nietch, C., Macke, D., … Su, H. (2016). Comparison of satellite reflectance algorithms for estimating chlorophyll-a in a temperate reservoir using coincident hyperspectral aircraft imagery and dense coincident surface observations. *Remote Sensing of Environment*, *178*, 15–30. https://doi.org/10.1016/j.rse.2016.03.002

Bélanger, S., Babin, M., & Larouche, P. (2008). An empirical ocean color algorithm for estimating the contribution of chromophoric dissolved organic matter to total light absorption in optically complex waters. *Journal of Geophysical Research*, *113*(C4), C04027. https://doi.org/10.1029/2007JC004436

Bramich, J., Bolch, C. J. S., & Fischer, A. (2021). Improved red-edge chlorophyll-a detection for Sentinel 2. *Ecological Indicators*, *120*, 106876. https://doi.org/10.1016/j.ecolind.2020.106876

Bricaud, A., Babin, M., Morel, A., & Claustre, H. (1995). Variability in the chlorophyll-specific absorption coefficients of natural phytoplankton: analysis and parameterization. *Journal of Geophysical Research*, *100*(C7), 13321–13332. https://doi.org/10.1029/95jc00463

Brockmann, C., Roland, Peters, M., Kerstin, Sabine, & Ruescas, A. (2016). *Evolution of the C2RCC neural network for Sentinel 2 and 3 for the reterieval of ocean colour products in normal and extreme optically complex waters.*

Campbell, G., Phinn, S. R., & Daniel, P. (2011). The specific inherent optical properties of three sub-tropical and tropical water reservoirs in Queensland, Australia. *Hydrobiologia*, *658*(1), 233–252. https://doi.org/10.1007/s10750-010-0476-4

Carpenter, D. J., & Carpenter, S. M. (1983). Modeling inland water quality using Landsat data. *Remote Sensing of Environment*, *13*(4), 345–352. https://doi.org/10.1016/0034-4257(83)90035-4

Chami, M., & Robilliard, D. (2002). Inversion of oceanic constituents in case I and II waters with genetic programming algorithms. *Applied Optics*, *41*(30), 6260. https://doi.org/10.1364/ao.41.006260

Chen, Jiang, Zhu, W., Tian, Y. Q., Yu, Q., Zheng, Y., & Huang, L. (2017). Remote estimation of colored dissolved organic matter and chlorophyll-a in Lake Huron using Sentinel-2 measurements. *Journal of Applied Remote Sensing*, *11*(03), 1. https://doi.org/10.1117/1.jrs.11.036007

Chen, Jun, Quan, W., & Cui, T. (2015). A Multi-Band Semi-Analytical Algorithm for Estimating Chlorophyll-a Concentration in the Yellow River Estuary, China. *Water Environment Research*, *87*(1), 44–51. https://doi.org/10.2175/106143014x14062131179032

Coble, P. G., Del Castillo, C. E., & Avril, B. (1998). Distribution and optical properties of CDOM in the Arabian Sea during the 1995 Southwest Monsoon. *Deep-Sea Research Part II: Topical Studies in Oceanography*, *45*(10–11), 2195–2223. https://doi.org/10.1016/S0967-0645(98)00068-X

Cohen, J. E. (1997). Estimates of Coastal Populations. *Science*, *278*(5341), 1209c – 1213. https://doi.org/10.1126/science.278.5341.1209c

Dan, S., Yu, C., Yuan-man, H., Tan, C., Lin-lin, J., Chun-lin, L., Ya-juan, S., & Tie-yu, W. (2015). *Landscape Pattern Change and Its Driving Forces in Liaoning Coastal Areas. 37*(5), 874–884. https://doi.org/10.13836/j.jjau.2015132

Danfen Zhou. (2015). Analysis of water Environment status and Pollution characteristics in Liaohe River Basin. *International Journal Hydroelectric Energy*. https://doi.org/CNKI:SUN:SZYB.0.2011-04-000

de Moraes Rudorff, N., & Kampel, M. (2012). Orbital remote sensing of phytoplankton functional types: A new review. In *International Journal of Remote Sensing* (Vol. 33, Issue 6, pp. 1967–1990). Taylor and Francis Ltd. https://doi.org/10.1080/01431161.2011.601343

Dong Dandan. (2020, January 12). *Using MODIS Data to Monitor the Spatial Distribution of Lake Chlorophyll-a.* Anhui Agricultural Science Bulletin. https://doi.org/1007-7731（2020）24-0150-02

Doxaran, D., Froidefond, J.-M., & Castaing, P. (2003). Remote-sensing reflectance of turbid sediment-dominated waters Reduction of sediment type variations and changing illumination conditions effects by use of reflectance ratios. *Applied Optics*, *42*(15), 2623. https://doi.org/10.1364/ao.42.002623

Duntley, S. Q. (1942). The Optical Properties of Diffusing Materials. *Journal of the Optical Society of America*, *32*(2), 61. https://doi.org/10.1364/josa.32.000061

Fan, H., Wang, X., Zhang, H., & Yu, Z. (2018). Spatial and temporal variations of particulate organic carbon in the Yellow-Bohai Sea over 2002-2016. In *Scientific Reports* (Vol. 8, Issue 1, p. 7971). Nature Publishing Group. https://doi.org/10.1038/s41598-018-26373-w

Gao Chen, Xu Jian, Gao Dan, Wang Lili, & Wang Yeqiao. (2019). *Retrieval of concentration of total suspended matter from GF-1 satellite and field measured spectral data during flood period in Poyang Lake.* Remote Sensing For Land & Resources. https://doi.org/10.6046/gtzyyg.2019.01.14

Giardino, C., Bresciani, M., Braga, F., Cazzaniga, I., De Keukelaere, L., Knaeps, E., & Brando, V. E. (2017). Bio-optical Modeling of Total Suspended Solids. In *Bio-optical Modeling and Remote Sensing of Inland Waters* (pp. 129–156). Elsevier Inc. https://doi.org/10.1016/B978-0-12-804644-9.00005-7

Gordon, H. R. (1988). A semianalytic radiance model of ocean color. *Journal of Geophysical Research*, *93*(D9), 10909–10924. https://doi.org/10.1029/JD093iD09p10909

Gordon, Howard R., & Morel, A. Y. (1983). *Remote Assessment of Ocean Color for Interpretation of Satellite Visible Imagery: A Review* (Vol. 4). American Geophysical Union. https://doi.org/10.1029/LN004

Gordon, Howard R., & Wang, M. (1994). Retrieval of water-leaving radiance and aerosol optical thickness over the oceans with SeaWiFS: a preliminary algorithm. *Applied Optics*, *33*(3), 443. https://doi.org/10.1364/ao.33.000443

Han, B., Loisel, H., Vantrepotte, V., Mériaux, X., Bryère, P., Ouillon, S., Dessailly, D., Xing, Q., & Zhu, J. (2016). Development of a Semi-Analytical Algorithm for the Retrieval of Suspended Particulate Matter from Remote Sensing over Clear to Very Turbid Waters. *Remote Sensing*, *8*(3), 211. https://doi.org/10.3390/rs8030211

Hoge, F. E., & Lyon, P. E. (1996). Satellite retrieval of inherent optical properties by linear matrix inversion of oceanic radiance models: An analysis of model and radiance measurement errors. *Journal of Geophysical Research: Oceans*, *101*(C7), 16631–16648. https://doi.org/10.1029/96JC01414

Johnsen, G., & Sakshaug, E. (2007). Biooptical characteristics of PSII and PSI in 33 species (13 pigment groups) of marine phytoplankton, and the relevance for pulseamplitude-modulated and fast-repetition-rate fluorometry. *Journal of Phycology*, *43*(6), 1236–1251. https://doi.org/10.1111/j.1529-8817.2007.00422.x

Jones, M. O. (2006). *Application of MODIS for monitoring water quality of a large Application of MODIS for monitoring water quality of a large oligotrophic lake oligotrophic lake.*

Kari, E., Kratzer, S., Beltrán-Abaunza, J. M., Harvey, E. T., & Vaičiūtė, D. (2017). Retrieval of suspended particulate matter from turbidity – model development, validation, and application to MERIS data over the Baltic Sea. *International Journal of Remote Sensing*, *38*(7), 1983–2003. https://doi.org/10.1080/01431161.2016.1230289

Kulkarni, A. (2011). Water quality retrieval from landsat TM imagery. *Procedia Computer Science*, *6*, 475–480. https://doi.org/10.1016/j.procs.2011.08.088

Kutser, T., Paavel, B., Kaljurand, K., Ligi, M., & Randla, M. (2019, February 4). Mapping Shallow Waters of the Baltic Sea with Sentinel-2 Imagery. *2018 IEEE/OES Baltic International Symposium, BALTIC 2018*. https://doi.org/10.1109/BALTIC.2018.8634850

Le, C., Lehrter, J. C., Hu, C., Schaeffer, B., MacIntyre, H., Hagy, J. D., & Beddick, D. L. (2015). Relation between inherent optical properties and land use and land cover across Gulf Coast estuaries. *Limnology and Oceanography*, *60*(3), 920–933. https://doi.org/10.1002/lno.10065

Lee, Z., Carder, K. L., & Arnone, R. A. (2002). Deriving inherent optical properties from water color: a multiband quasi-analytical algorithm for optically deep waters. *Applied Optics*, *41*(27), 5755. https://doi.org/10.1364/ao.41.005755

Liang, X. W., Shao, T. T., & Wang, T. (2020). CDOM Optical Characteristics and Related Environmental Factors of High-turbidity Waters on the Loess Plateau. *Huanjing Kexue/Environmental Science*, *41*(3), 1217–1226. https://doi.org/10.13227/j.hjkx.201908244

Lin, J., Lee, Z., Ondrusek, M., & Liu, X. (2009). Hyperspectral absorption and backscattering coefficients of bulk water retrieved from a combination of remote-sensing reflectance and attenuation coefficient "A model for the diffuse attenuation coefficient of downwelling irradiance. *Journal of Geophysical Research: Oceans*, *30*(2), 2016. https://doi.org/10.1364/OE.26.00A157

Maritorena, S., Siegel, D. A., & Peterson, A. R. (2002). Optimization of a semianalytical ocean color model for global-scale applications. *Applied Optics*, *41*(15), 2705. https://doi.org/10.1364/ao.41.002705

Mobely, C. D. (1994). *Light and Water: Radiative Transfer in Natural Waters*. Academiv Press.

Mohamed, M. F. (2015). Satellite data and real time stations to improve water quality of Lake Manzalah. *Water Science*, *29*(1), 68–76. https://doi.org/10.1016/j.wsj.2015.03.002

Nana Feng. (2020). Effect of land use pattern on water quality in Liaohe Conservation Area. *Journal of Environmental Engineering Technology*, 579–584. https://doi.org/10.12153/j.issn.1674-991X.20200029

Nechad, B., Ruddick, K. G., & Park, Y. (2010). Calibration and validation of a generic multisensor algorithm for mapping of total suspended matter in turbid waters. *Remote Sensing of Environment*, *114*(4), 854–866. https://doi.org/10.1016/j.rse.2009.11.022

Ngoc, D. D., Loisel, H., Vantrepotte, V., Chu Xuan, H., Nguyen Minh, N., Verpoorter, C., Meriaux, X., Pham Thi Minh, H., Le Thi, H., Le Vu Hong, H., & Nguyen Van, T. (2020). A Simple Empirical Band-Ratio Algorithm to Assess Suspended Particulate Matter from Remote Sensing over Coastal and Inland Waters of Vietnam: Application to the VNREDSat-1/NAOMI Sensor. *Water*, *12*(9), 2636. https://doi.org/10.3390/w12092636

Pope, R. M., & Fry, E. S. (1997). Absorption spectrum (380–700 nm) of pure water II Integrating cavity measurements. *Applied Optics*, *36*(33), 8710. https://doi.org/10.1364/ao.36.008710

Qi, Y., Sun, Y. G., Ma, G. B., Wu, N., & Fu, Y. Bin. (2020). Temporal and Spatial Variation Patterns of the Environmental Elements in the Sediments of the Liaohe Estuary and the Related Influencing Factors. *Huanjing Kexue/Environmental Science*, *41*(7), 3175–3185. https://doi.org/10.13227/j.hjkx.201910041

Ronghua, M., Junwu, T., Hongtao, D., & Delu, P. (2009). Progress in lake water color remote sensing. *Journal of Lake Sciences*, *21*(2), 143–158. https://doi.org/10.18307/2009.0201

Salama, M. S., & Shen, F. (2010). Stochastic inversion of ocean color data using the cross-entropy method. *Optics Express*, *18*(2), 479. https://doi.org/10.1364/oe.18.000479

Salama, M. S., & Verhoef, W. (2015). Two-stream remote sensing model for water quality mapping: 2SeaColor. *Remote Sensing of Environment*, *157*, 111–122. https://doi.org/10.1016/j.rse.2014.07.022

Shan, J., Yicheng, W., & Renfeng, M. (n.d.). Change conalysis of chlorophyll concentration in the East China Sea and its response to seawater temperature. *Bulletin of Surveying and Mapping*, *0*(6), 39. https://doi.org/10.13474/J.CNKI.11-2246.2020.0177

SHAO Zhi-Fang, HU Hong, LI Zheng-Yan, & ZHENG Yun-Yun. (2015). Set Pair Analysis Model for Daliao River Estuarine Water Ecosystem Health Assessment. *Periodical of Ocean University of China*, *3*, 18–27. https://doi.org/10.16441/j.cnki.hdxb.20130439

Siswanto, E., Tang, J., Yamaguchi, H., Ahn, Y. H., Ishizaka, J., Yoo, S., Kim, S. W., Kiyomoto, Y., Yamada, K., Chiang, C., & Kawamura, H. (2011). Empirical ocean-color algorithms to retrieve chlorophyll-a, total suspended matter, and colored dissolved organic matter absorption coefficient in the Yellow and East China Seas. *Journal of Oceanography*, *67*(5), 627–650. https://doi.org/10.1007/s10872-011-0062-z

Song, Y., Liu, R., Sun, Y., Lei, K., & Kolditz, O. (2015). Waste water treatment and pollution control in the Liao River Basin. In *Environmental Earth Sciences* (Vol. 73, Issue 9, pp. 4875–4880). Springer Verlag. https://doi.org/10.1007/s12665-015-4333-7

Tassan, S. (1994). Local algorithms using SeaWiFS data for the retrieval of phytoplankton, pigments, suspended sediment, and yellow substance in coastal waters. *Applied Optics*, *33*(12), 2369. https://doi.org/10.1364/ao.33.002369

Tian Hongzhen, Liu Qinping, Joaquim, Goes, Helga do Rosario Gomes, & Yang Mengmeng. (2019). *Temporal and spatial changes in chlorophyll a concentrations in the Bohai Sea in the past two decades*. Haiyang Xuebao. https://doi.org/10.3969/j.issn.0253-4193.2019.08.015

Vanhellemont, Q. (2019). Adaptation of the dark spectrum fitting atmospheric correction for aquatic applications of the Landsat and Sentinel-2 archives. *Remote Sensing of Environment*, *225*, 175–192. https://doi.org/10.1016/j.rse.2019.03.010

Wang, Y., Shen, F., Sokoletsky, L., & Sun, X. (2017). Validation and Calibration of QAA Algorithm for CDOM Absorption Retrieval in the Changjiang (Yangtze) Estuarine and Coastal Waters. *Remote Sensing*, *9*(11), 1192. https://doi.org/10.3390/rs9111192

Wu, W. G., Zhang, J. H., Wang, W., Li, J. Q., Fang, J. H., Liu, Y., Gao, Z. K., Zhang, Y. T., & Chen, J. (2016). Distribution of chlorophyll-a concentration and its control factors in spring in Sungo Bay. *Shengtai Xuebao/ Acta Ecologica Sinica*, *36*(15), 4855–4863. https://doi.org/10.5846/stxb201501130102

Xiaowei Zhang. (2014). Analysis of comprehensive water quality variation trend of Daliao River Estuary. *Shaanxi Water Resources*, *1*. https://doi.org/10.3969/j.issn.1673-9000.2014.01.071

Xu, K., & Fan, Z. (2018). *Relationship between chlorophyll-a and temperature, pH and transparency in water quality monitoring of Yuxiba Reservoir*. Inner Mongolia Environmental Sciences. https://doi.org/10.16647/j.cnki.cn15-1369/X.2018.08.090

Yu, X., Salama, M. S., Shen, F., & Verhoef, W. (2016). Retrieval of the diffuse attenuation coefficient from GOCI images using the 2SeaColor model: A case study in the Yangtze Estuary. *Remote Sensing of Environment*, *175*, 109–119. https://doi.org/10.1016/j.rse.2015.12.053

Zhang, Y.-L., Bo-Qiang, Q., Rong-Hua, M. A., Guang-W Ei, Z. U., Zhang, L., & We-I Min, C. (n.d.). *Chromophoric Dissolved Organic Matter Absorption Characteristics with Relation to Fluorescence in Typical Macrophyte, Algae Lake Zones of Lake Taihu*.

Zhang, Y., Qin, B., Zhu, G., Zhang, L., & Yang, L. (2007). Chromophoric dissolved organic matter (CDOM) absorption characteristics in relation to fluorescence in Lake Taihu, China, a large shallow subtropical lake. *Hydrobiologia*, *581*(1), 43–52. https://doi.org/10.1007/s10750-006-0520-6

Zhao, H., Li, Q., & Tao, J. (2016). Spatio-temporal water quality variations and identification of surface water pollutant sources in Bohai Bay. *Shuili Fadian Xuebao/Journal of Hydroelectric Engineering*, *35*(10), 21–30. https://doi.org/10.11660/slfdxb.20161003

Zhao, N., Zhang, G., Zhang, S., Bai, Y., Ali, S., & Zhang, J. (2019). Temporal-Spatial Distribution of Chlorophyll-a and Impacts of Environmental Factors in the Bohai Sea and Yellow Sea. *IEEE Access*, *7*, 160947–160960. https://doi.org/10.1109/ACCESS.2019.2950833

ZHAO Xue, LIU Dawei, LI Jiacun, GONG Xiaojian, & HU Ke. (2018). Evolution of Modern Sedimentary Bodies of Liaohe Estuary Delta Based on Remote-Sensing Method. *Ocean Development and Management* . https://doi.org/10.3969/j.issn.1005-9857.2018.01.013

Zheng Shuxian, Huang Binbin, & Dai Ming. (2019). *Effect of Sediment Suspension on Phytoplankton Growth*. Transactions of Oceanology and Limnology. https://doi.org/CNKI:SUN:HYFB.0.2020-01-019

Zhu, W., Yu, Q., Tian, Y. Q., Chen, R. F., & Gardner, G. B. (2011). Estimation of chromophoric dissolved organic matter in the Mississippi and Atchafalaya river plume regions using above-surface hyperspectral remote sensing. *Journal of Geophysical Research*, *116*(C2), C02011. https://doi.org/10.1029/2010JC006523